Supply chain loss from easing COVID-19 restrictions: an evolutionary epidemiological-economic modeling study

Yang Ye[1,4], Zhidong Cao[2], Daniel Dajun Zeng[2,*], Qingpeng Zhang[1,3,4,*]

Supplementary Note 1: Modeling the effectiveness of NPIs on local and international transmission

The effectiveness of NPIs on international transmission, denoted by $\hat{\gamma}_i(t) \in [0, 1]$ for country i at time t, is captured by the reduction in international movement compared to the pre-pandemic level. Then,

$$G_{ij}(t) = G_{ji}(t) = \overline{G}_{ij} \min\{1 - \hat{\gamma}_i(t), 1 - \hat{\gamma}_j(t)\}, \tag{S1}$$

where $\overline{G}_{ij}$ is the number of individuals travelling between country i and country j before the pandemic. After full reopening, $\hat{\gamma}_i(t) = 0$. To model how countries introduce and relax NPIs to control local transmission before full reopening, we consider the local effective reproduction number-based adaptive policy adoption strategy, which is represented by the following sigmoidal function with shape parameter k:

$$c_i(t) = c_i^{mild}(t) + \frac{c_i^{stringent}(t) - c_i^{mild}(t)}{1 + e^{k[1 - R_{e,i}(t)]}}. \tag{S2}$$

Here, $R_{e,i}(t)$ is the local effective reproduction number for country i at time t; $c_i^{stringent}(t)$ and $c_i^{mild}(t)$ are the effectiveness of the most stringent and mildest NPIs implemented by country i at time t. After full reopening, $c_i(t) = 0$.

$R_{e,i}(t)$ is computed as the dominant eigenvalue of the Next Generation Matrix (NGM) associated with the dynamical system considered. The local disease transmission dynamics within country i (when it is isolated from the metapopulation network) are represented by the following equations:

$$\begin{aligned}
\partial_t S_i(t) &= \Lambda_i(t) - \phi_i(t) N_i - \lambda_i^S(t) S_i(t) + \varepsilon V_i(t) + \psi R_i(t) - \upsilon S_i(t),\\
\partial_t V_i(t) &= \phi_i(t) N_i - \lambda_i^V(t) V_i(t) - \varepsilon V_i(t) - \upsilon V_i(t),\\
\partial_t E_i^S(t) &= \lambda_i^S(t) S_i(t) - \sigma E_i^S(t) - \upsilon E_i^S(t),\\
\partial_t E_i^V(t) &= \lambda_i^V(t) V_i(t) - \sigma E_{i,m}^V(t) - \upsilon E_i^V(t),\\
\partial_t I_i^S(t) &= \sigma E_i^S(t) - \alpha I_i^S(t) - \upsilon I_i^S(t),\\
\partial_t I_i^V(t) &= \sigma E_i^V(t) - \alpha I_i^V(t) - \upsilon I_i^V(t),\\
\partial_t R_i(t) &= (1 - \nu)\alpha I_i^S(t) + [1 - (1 - \epsilon)\nu]\alpha I_i^V(t) - \psi R_i(t) - \upsilon R_i(t),\\
\partial_t D_i(t) &= \nu\alpha I_i^S(t) + (1 - \epsilon)\nu\alpha I_i^V(t).
\end{aligned} \tag{S3}$$

This system has 4 infected states (E_i^S, E_i^V, I_i^S, and I_i^V). The infected subsystem is

$$\begin{aligned}
\partial_t E_i^S(t) &= \lambda_i^S(t) S_i(t) - \sigma E_i^S(t) - \upsilon E_i^S(t),\\
\partial_t E_i^V(t) &= \lambda_i^V(t) V_i(t) - \sigma E_{i,m}^V(t) - \upsilon E_i^V(t),\\
\partial_t I_i^S(t) &= \sigma E_i^S(t) - \alpha I_i^S(t) - \upsilon I_i^S(t),\\
\partial_t I_i^V(t) &= \sigma E_i^V(t) - \alpha I_i^V(t) - \upsilon I_i^V(t),
\end{aligned}$$

The infected subsystem is composed by the state variable $x = [E_i^S, E_i^V, I_i^S, I_i^V]$. Then, we can construct the transmission term $\mathbf{V_{F,i}}$ and the transition term $\mathbf{V_{F,i}}$ as follows.

$$\mathbf{V_{F,i}} = \begin{bmatrix} [1-c_i(t)]\beta\frac{I_i^S(t)+I_i^V(t)}{N_i}S_i(t) \\ [1-c_i(t)](1-\eta)\beta\frac{I_i^S(t)+I_i^V(t)}{N_i}V_i(t) \\ 0 \\ 0 \end{bmatrix},$$

and

$$\mathbf{V_{V,i}} = \begin{bmatrix} (\sigma+\upsilon)E_i^S \\ (\sigma+\upsilon)E_i^V \\ \alpha I_i^S - (\sigma+\upsilon)E_i^S \\ \alpha I_i^V - (\sigma+\upsilon)E_i^V \end{bmatrix}.$$

Hence, the transmission matrix $\mathbf{M_{F,i}}$ and the transition matrix $\mathbf{M_{V,i}}$ become

$$\mathbf{M_{F,i}} = \begin{bmatrix} 0 & 0 & (1-c_i)\beta S_i/N_i & (1-c_i)\beta S_i/N_i \\ 0 & 0 & (1-c_i)(1-\eta)\beta V_i/N_i & (1-c_i)(1-\eta)\beta V_i/N_i \\ 0 & 0 & 0 & 0 \\ 0 & 0 & 0 & 0 \end{bmatrix},$$

and

$$\mathbf{M_{V,i}} = \begin{bmatrix} \sigma+\upsilon & 0 & 0 & 0 \\ 0 & \sigma+\upsilon & 0 & 0 \\ -(\sigma+\upsilon) & 0 & \alpha & 0 \\ 0 & -(\sigma+\upsilon) & 0 & \alpha \end{bmatrix},$$

Therefore, the next generation matrix for country i is given by

$$\begin{aligned} NGF_i &= \mathbf{M_{F,i}}\mathbf{M_{V,i}}^{-1} \\ &= \begin{bmatrix} 0 & 0 & (1-c_i)\beta S_i/N_i & (1-c_i)\beta S_i/N_i \\ 0 & 0 & (1-c_i)(1-\eta)\beta V_i/N_i & (1-c_i)(1-\eta)\beta V_i/N_i \\ 0 & 0 & 0 & 0 \\ 0 & 0 & 0 & 0 \end{bmatrix} \begin{bmatrix} 1/(\sigma+\upsilon) & 0 & 0 & 0 \\ 0 & 1/(\sigma+\upsilon) & 0 & 0 \\ 1/\alpha & 0 & 1/\alpha & 0 \\ 0 & 1/\alpha & 0 & 1/\alpha \end{bmatrix} \\ &= \frac{(1-c_i)\beta}{\alpha N_i} \begin{bmatrix} S_i & S_i & S_i & S_i \\ (1-\eta)V_i & (1-\eta)V_i & (1-\eta)V_i & (1-\eta)V_i \\ 0 & 0 & 0 & 0 \\ 0 & 0 & 0 & 0 \end{bmatrix}. \end{aligned}$$

The local effective reproduction number of country i is the dominant eigenvalue of NGF_i, which is $\frac{(1-c_i)\beta}{\alpha N_i}[(1-\eta)V_i + S_i]$.

Currently, many countries have largely reopened. Even China, one of the countries maintaining stringent COVID-19 policies, eased its zero-COVID policy on November 11, 2022, so we assume that all countries will no long relax the remaining COVID-19 restrictions after November 11, 2022, until full reopening. The CHI score for each country before November 11, 2022, is obtained from the Oxford COVID-19 Government Response Tracker [1]. We assume that $c_i^{stringent}(t)$, $c_i^{mild}(t)$, and $\hat{\gamma}_i(t)$ for country i are linearly associated with its CHI score $CHI_i(t)$, i.e.,

$$\begin{aligned} c_i^{stringent}(t) &= a_1 CHI_i(t) + b_1, \\ c_i^{mild}(t) &= a_2 CHI_i(t) + b_2, \\ \hat{\gamma}_i(t) &= a_3 CHI_i(t) + b_3. \end{aligned}$$

For countries lifting all COVID-19 restrictions, $c_i^{stringent}(t) = c_i^{mild}(t) = \hat{\gamma}_i(t) = CHI_i(t) = 0$. Then, $b_1 = b_2 = b_3 = 0$. We denote the values of $c_i^{stringent}(t)$, $c_i^{mild}(t)$, $\hat{\gamma}_i(t)$, and $CHI_i(t)$ for China on April 15, 2022 as $c_{\text{CHN}}^{stringent}$, c_{CHN}^{mild}, $\hat{\gamma}_{\text{CHN}}$, CHI_{CHN} respectively. Then,

$$\begin{aligned} a1 &= c_{\text{CHN}}^{stringent}/CHI_{CHN}, \\ a2 &= c_{\text{CHN}}^{mild}/CHI_{CHN}, \\ a3 &= \hat{\gamma}_{\text{CHN}}/CHI_{CHN}. \end{aligned}$$

The values of $c_{\mathrm{CHN}}^{stringent}$ and c_{CHN}^{mild} are inferred from real-world and real-time data in Shanghai, China [2]. The value of $\hat{\gamma}_{\mathrm{CHN}}$ is obtained from OAG [3]. See parameter values in Supplementary Table 4.

Supplementary Note 2: The change in gross value added

The pre-pandemic, maximum, and actual GVA for firm ai at time t are represented by $x_{ai}^{*}q_{ai}^{L}$ (i.e., L_{ai}^{*}), $L_{ai}(t)$, and $x_{ai}^{A}(t)q_{ai}^{L}$, respectively. The total GVA change for firm ai at time t relative to the pre-pandemic level is represented by

$$\Delta GVA_{ai}^{total}(t) = \frac{x_{ai}^{A}(t)q_{ai}^{L} - x_{ai}^{*}q_{ai}^{L}}{x_{ai}^{*}q_{ai}^{L}} = \frac{x_{ai}^{A}(t)}{x_{ai}^{*}} - 1.$$

We define the pandemic-induced GVA change as the change in labour input due to illness or COVID-19 restrictions on economic activities. Thus,

$$\Delta GVA_{ai}^{pandemic}(t) = \frac{L_{ai}(t)/\kappa_{ai}(t)}{L_{ai}^{*}} - 1$$

represents the pandemic-induced GVA change for firm ai at time t relative to the pre-pandemic level. We define the competition-induced GVA change as the change in production capacity due to competition between firms. Thus,

$$\Delta GVA_{ai}^{competition}(t) = \frac{L_{ai}(t) - L_{ai}^{*}}{L_{ai}^{*}} - \Delta GVA_{ai}^{direct}(t)$$

represents the competition-induced GVA change for firm ai at time t relative to the pre-pandemic level. Then, the supply disruption-induced indirect GVA change for firm ai at time t relative to the pre-pandemic level is represented by

$$\Delta GVA_{ai}^{supply}(t) = \Delta GVA_{ai}^{total}(t) - \Delta GVA_{ai}^{pandemic}(t) - \Delta GVA_{ai}^{competition}(t).$$

Supplementary Note 3: Market structure change regression

We present details of the regression results reported in Table 1 in the main text. We use the Ordinary Least Squares linear regression model to estimate the relative role of hypothesized factors on market structure changes for different sectors. We consider three dependent variables: sectors' market structure changes over the projection horizon under three global reopening scenarios. Denote the market structure change over the projection horizon for sector a as $\Delta\mathcal{M}_a$. We define

$$\Delta\mathcal{M}_a = \sum_i [M_{ai}(T) - M_{ai}(0)]^2, \tag{S4}$$

where $M_{ai}(t)$ represents the market share of firm ai at time t, T is the length of the projection horizon. $\Delta\mathcal{M}_a^{\mathrm{Early}}$, $\Delta\mathcal{M}_a^{\mathrm{Moderate}}$, and $\Delta\mathcal{M}_a^{\mathrm{Late}}$ represent the market structure changes for sector a under the early, moderate, and late full-reopening scenarios, respectively. We separately test the distribution of market structure changes over the projection horizon among sectors under each global reopening scenario. Results show that under all reopening scenarios, sectors' market structure changes over the projection horizon follow a log-normal distribution (Supplementary Figure 1). To reduce skewness, we use log transformation to normalize dependent variables.

We investigate four hypotheses. The first hypothesis is that the variations in market structure changes among sectors result from the heterogeneous impacts of COVID-19 restrictions on production and final demand. The model includes two such independent variables: the impact-to-labour multiplier (ϑ_a^P) and the impact-to-demand multiplier (ϑ_a^D). The second hypothesis is that sectors with a larger diversity in exposure to supply chain risks among firms are more likely to experience larger market structure changes. We propose a metric, namely, risk diversity, to measure this factor. A firm's exposure to supply chain risks is defined by multiplying its market share before the pandemic by the CHI score of the country in which it is located. We quantify diversity based on Shannon entropy. Thus, the risk diversity of sector a is calculated as

$$\sum_i p_{ai} \log p_{ai}, \tag{S5}$$

where

$$p_{ai} = \frac{M_{ai}(0)CHI_i}{\sum_j M_{aj}(0)CHI_j},$$

represents the normalized exposure to supply chain risks of firm ai. Sectors where production hubs are located in highly restrictive countries have larger values of risk diversity (Supplementary Figure 3). The third hypothesis is that the market structure change of a sector is associated with its degree of self-reliance. We use the fraction of self-supplied demand to measure this factor, which is defined as

$$\frac{\sum_j Z^*_{aj \to ai}}{\sum_j \sum_b Z^*_{bj \to ai}}$$

for sector a. The fourth hypothesis is that the market structure change of a sector is associated with its topological position on the global supply network [4]. To measure this factor, we construct a sector dependency network, where a node represents a sector, and an edge represents the total trade flow between two sectors before the pandemic. We use the eigenvector centrality [5] of a sector on the sector dependency network in this hypothesis in the main text. We also consider the betweenness centrality and the degree of a sector in this note. They are defined as follows.

- Betweenness centrality [6]: the extent to which a sector lies on the shortest paths between other sectors on the sector dependency network
- Degree: the number of edges (excluding the self-loop edge) of a sector on the sector dependency network

Each independent variable is normalized by subtracting the mean and dividing by the standard deviation. The distribution of each independent variable is presented in Supplementary Figure 2. We report the pair-wise Pearson and Spearman correlation coefficients of independent variables in Supplementary Table 1. All correlation coefficients are lower than 0.5 except except the correlation coefficient between the eigenvector centrality and degree, indicating that the independent variables are generally weakly correlated. Due to the high correlation between degree, betweenness centrality, and eigenvector centrality, we consider three sets of regression models, each of which includes one independent variable of them. Regression models including the eigenvector centrality generate the best result, thus, are presented in the main text. Other regression models are presented in the Supplementary Tables 2 and 3.

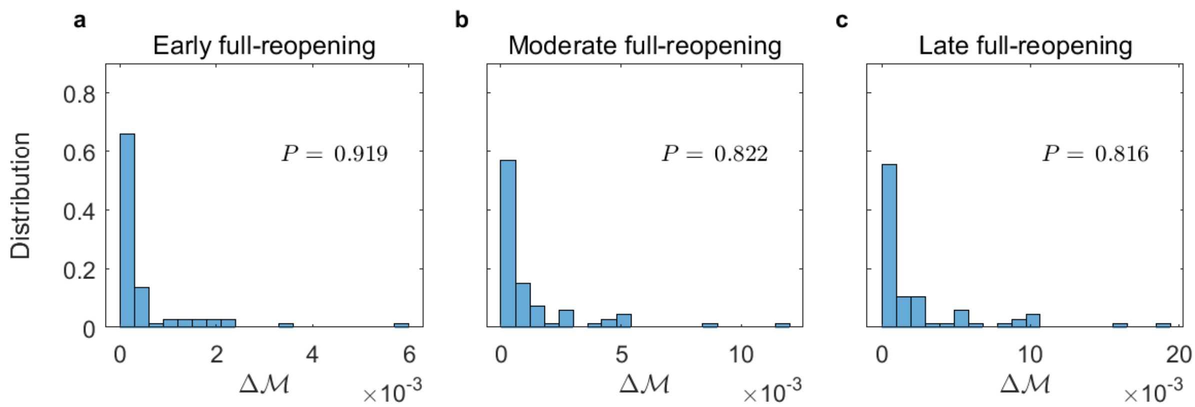

Supplementary Figure 1: Distribution of market structure changes over the projection horizon among sectors under different global reopening scenarios. **a**, The early full-reopening scenario. **b**, The moderate full-reopening scenario. **c**, The late full-reopening scenario. $\Delta\mathcal{M}$, Market structure changes over the projection horizon. A two-sided Kolmogorov–Smirnov (KS) test is performed to assess whether market structure changes among production sectors follow a log-normal distribution. The figure in each panel is the KS test P value. The smallest KS test P value is 0.816, indicating that the distribution of market structure changes among production sectors can be well fitted by the log-normal distribution.

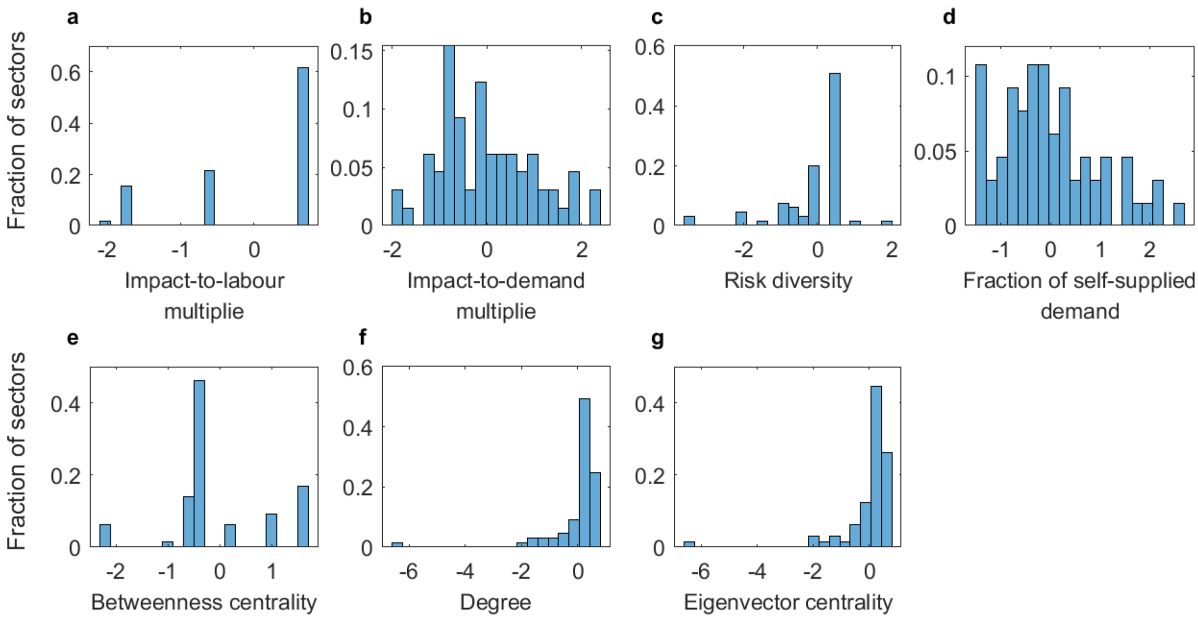

Supplementary Figure 2: The distribution of normalized independent variables.

Supplementary Table 1: Pairwise Pearson and Spearman correlation coefficients of independent variables

	ϑ^P	ϑ^D	Risk diversity	Fraction of self-supplied demand	Betweenness centrality	Degree	Eigenvector centrality
ϑ^P	1	-0.304	0.185	0.172	0.24	0.036	0.03
ϑ^D	-0.304	1	-0.102	-0.124	-0.123	-0.194	-0.192
Risk diversity	0.185	-0.102	1	0.405	0.148	-0.013	-0.014
Fraction of self-supplied demand	0.172	-0.124	0.405	1	0.138	0.261	0.261
Betweenness centrality	0.24	-0.123	0.148	0.138	1	0.47	0.445
Degree	0.036	-0.194	-0.013	0.261	0.47	1	1
Eigenvector centrality	0.03	-0.192	-0.014	0.261	0.445	1	1

Supplementary Table 2: Regression analysis of variables associated with sectors' market structure changes (with degree)

Independent variables	$ln\Delta\mathcal{M}^{\text{Early}}$	$ln\Delta\mathcal{M}^{\text{Moderate}}$	$ln\Delta\mathcal{M}^{\text{Late}}$
Impact-to-labour multiplier (ϑ^P)	1.041 (0.212)***	0.994 (0.218)***	1.013 (0.213)***
Impact-to-demand multiplier (ϑ^D)	0.156 (0.212)	0.132 (0.218)	0.119 (0.213)
Risk diversity	0.685 (0.22)***	0.736 (0.227)***	0.709 (0.222)***
e Fraction of self-supplied demand	0.689 (0.227)***	0.609 (0.234)**	0.586 (0.228)**
Degree	−0.222 (0.211)	−0.274 (0.217)	−0.271 (0.212)
No. Observations	65	65	65
R^2	0.542	0.515	0.521
Adjusted R^2	0.503	0.474	0.481
F-statistic	13.963***	12.522***	12.842***
Residual Shapiro-Wilks p	0.068*	0.049**	0.019**

$ln\Delta\mathcal{M}^{\text{Early}}$, $ln\Delta\mathcal{M}^{\text{Moderate}}$, and $ln\Delta\mathcal{M}^{\text{Late}}$ represent the logarithm of sectors' changes in market structure over the projection horizon under the early, moderate, and late full-reopening scenarios, respectively. R^2, the square of the Pearson correlation coefficient. The normality of residuals is evaluated by the Shapiro-Wilks test. Figures in parentheses are standard errors of the coefficient. *Significant at the 10% level; **significant at the 5% level; ***Significant at the 1% level.

Supplementary Table 3: Regression analysis of variables associated with sectors' market structure changes (with betweenness)

Independent variables	$ln\Delta\mathcal{M}^{\text{Early}}$	$ln\Delta\mathcal{M}^{\text{Moderate}}$	$ln\Delta\mathcal{M}^{\text{Late}}$
Impact-to-labour multiplier (ϑ^P)	0.99 (0.213)***	0.948 (0.22)***	0.972 (0.216)***
Impact-to-demand multiplier (ϑ^D)	0.209 (0.206)	0.195 (0.214)	0.179 (0.21)
Risk diversity	0.693 (0.216)***	0.753 (0.224)***	0.728 (0.22)***
Fraction of self-supplied demand	0.591 (0.215)***	0.495 (0.223)**	0.476 (0.219)**
Betweenness centrality	0.322 (0.203)	0.313 (0.21)	0.283 (0.206)
No. Observations	65	65	65
R^2	0.552	0.52	0.523
Adjusted R^2	0.514	0.479	0.483
F-statistic	14.562***	12.773***	12.944***
Residual Shapiro-Wilks p	0.166	0.042**	0.016**

$ln\Delta\mathcal{M}^{\text{Early}}$, $ln\Delta\mathcal{M}^{\text{Moderate}}$, and $ln\Delta\mathcal{M}^{\text{Late}}$ represent the logarithm of sectors' changes in market structure over the projection horizon under the early, moderate, and late full-reopening scenarios, respectively. R^2, the square of the Pearson correlation coefficient. The normality of residuals is evaluated by the Shapiro-Wilks test. Figures in parentheses are standard errors of the coefficient. *Significant at the 10% level; **significant at the 5% level; ***Significant at the 1% level.

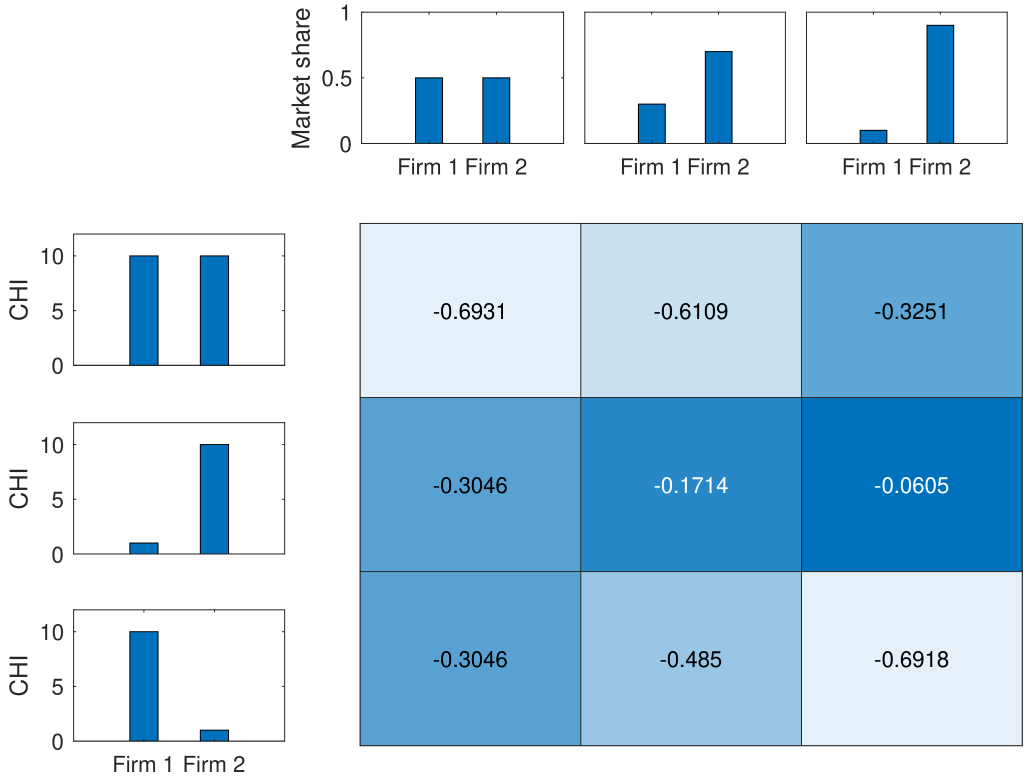

Supplementary Figure 3: The risk diversity values of sectors with varying marker structures and CHI values among firms. We assume there are only two firms in a sector. We observe a higher risk diversity in the sector where the larger firm is located in the country with a higher CHI value.

Supplementary Note 4: Model parameter settings

The model works in a weekly time step. In the main text, we set $\phi_i = 0.01\text{day}^{-1}$, $k = 100$, $\rho = 0.01$, $\varphi = 0.7$, $n_{ai} = 3$, and $I_{thre} = 1e - 3$. Since no data is available to inform the values of these parameters, we perform comprehensive sensitivity analyses to examine the impact of these baseline assumptions on the main results (Supplementary Figures 16-23). The values of other parameters are informed by existing literature (Supplementary Table 4). We do not consider the mutation of the virus. We set the transmissibility of the virus based on data of the currently circulating variant of concern-Omicron (`https://www.who.int/activities/tracking-SARS-CoV-2-variants`). We define vaccinated individuals as those who have received a booster dose after completing the initial vaccination protocol (two doses). We set the efficacy of vaccines based on the efficacy of a booster dose.

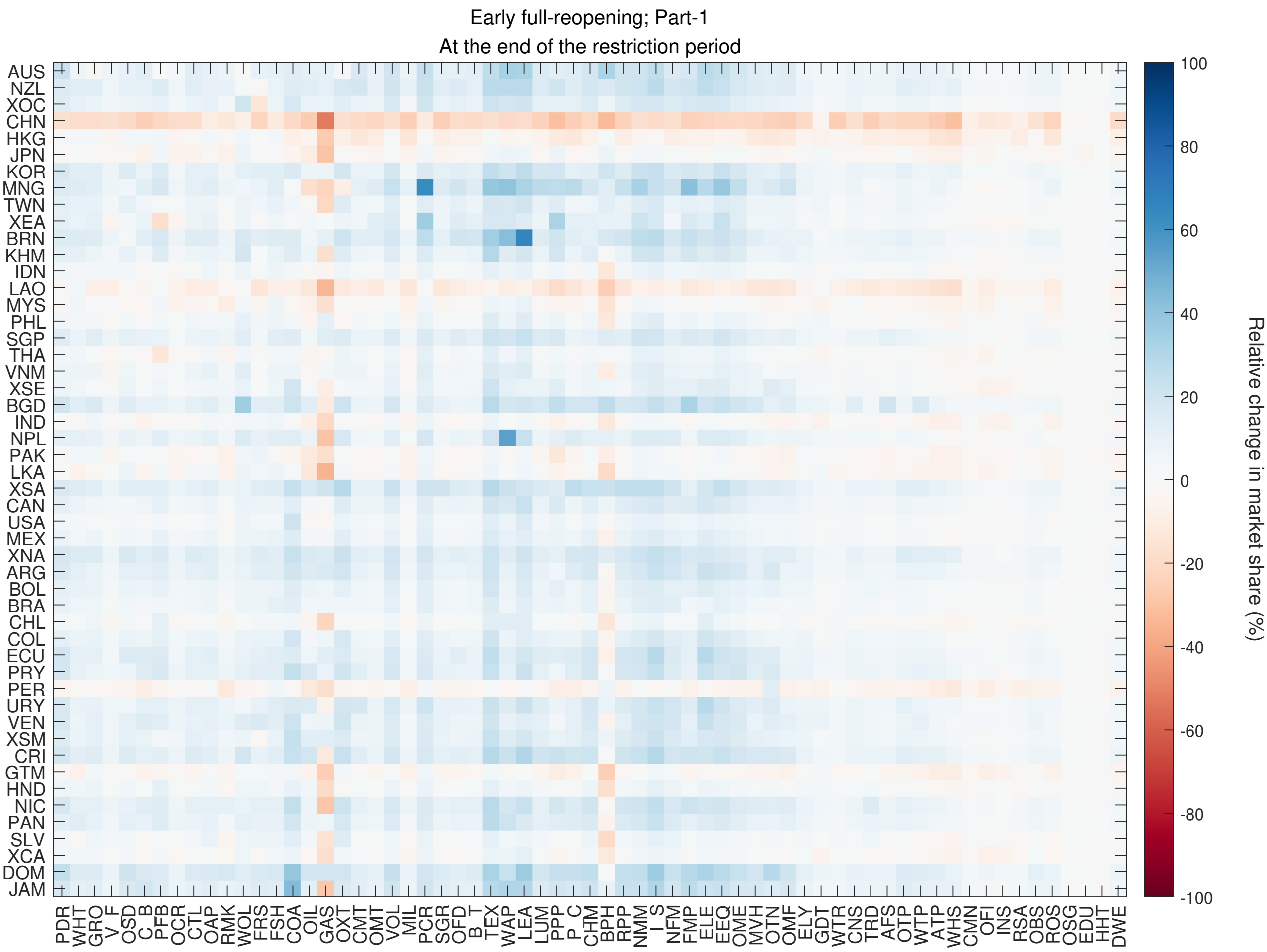

Supplementary Figure 4: Each country/region's changes in market share relative to the pre-pandemic level by sectors at the end of the restriction period under the early full-reopening scenario. Countries and sectors are presented with three-letter codes. The description of country/region and sector codes can be found in Supplementary tables 6-7.

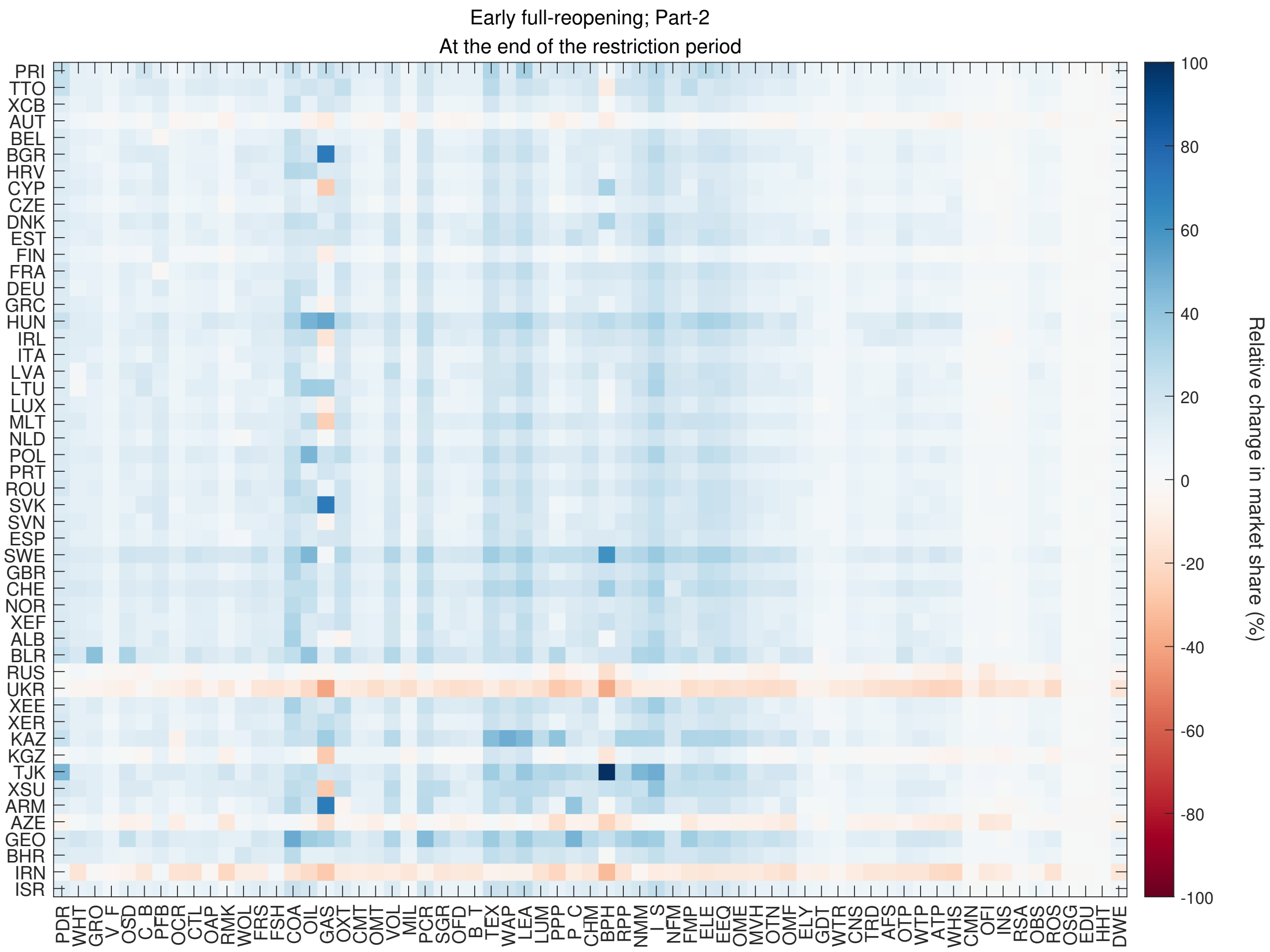

Supplementary Figure 5: Each country/region's changes in market share relative to the pre-pandemic level by sectors at the end of the restriction period under the early full-reopening scenario. Countries/regions and sectors are presented with three-letter codes. The description of country/region and sector codes can be found in Supplementary tables 6-7.

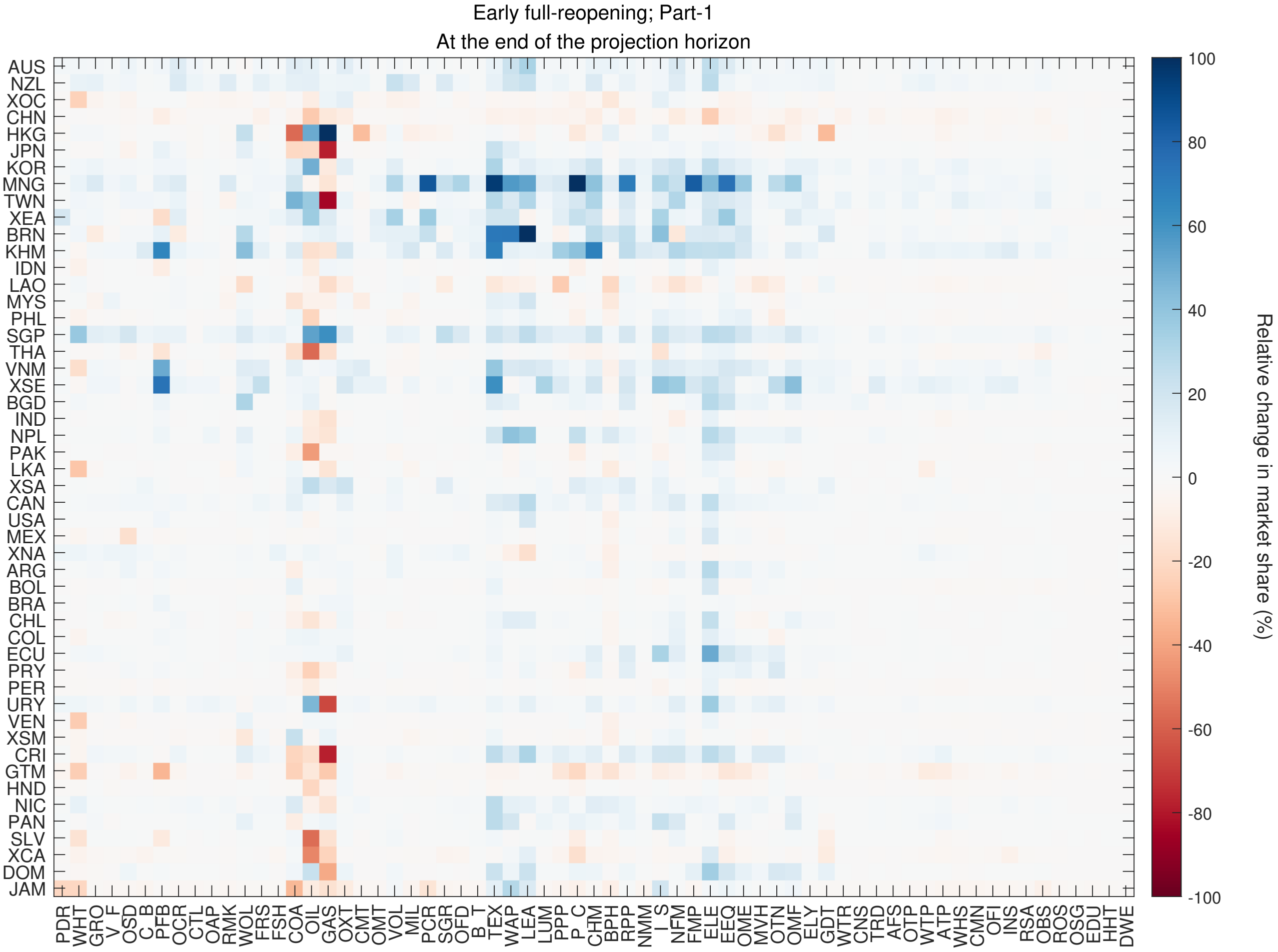

Supplementary Figure 6: Each country/region's changes in market share relative to the pre-pandemic level by sectors at the end of the projection horizon under the early full-reopening scenario. Countries/regions and sectors are presented with three-letter codes. The description of country/region and sector codes can be found in Supplementary tables 6-7.

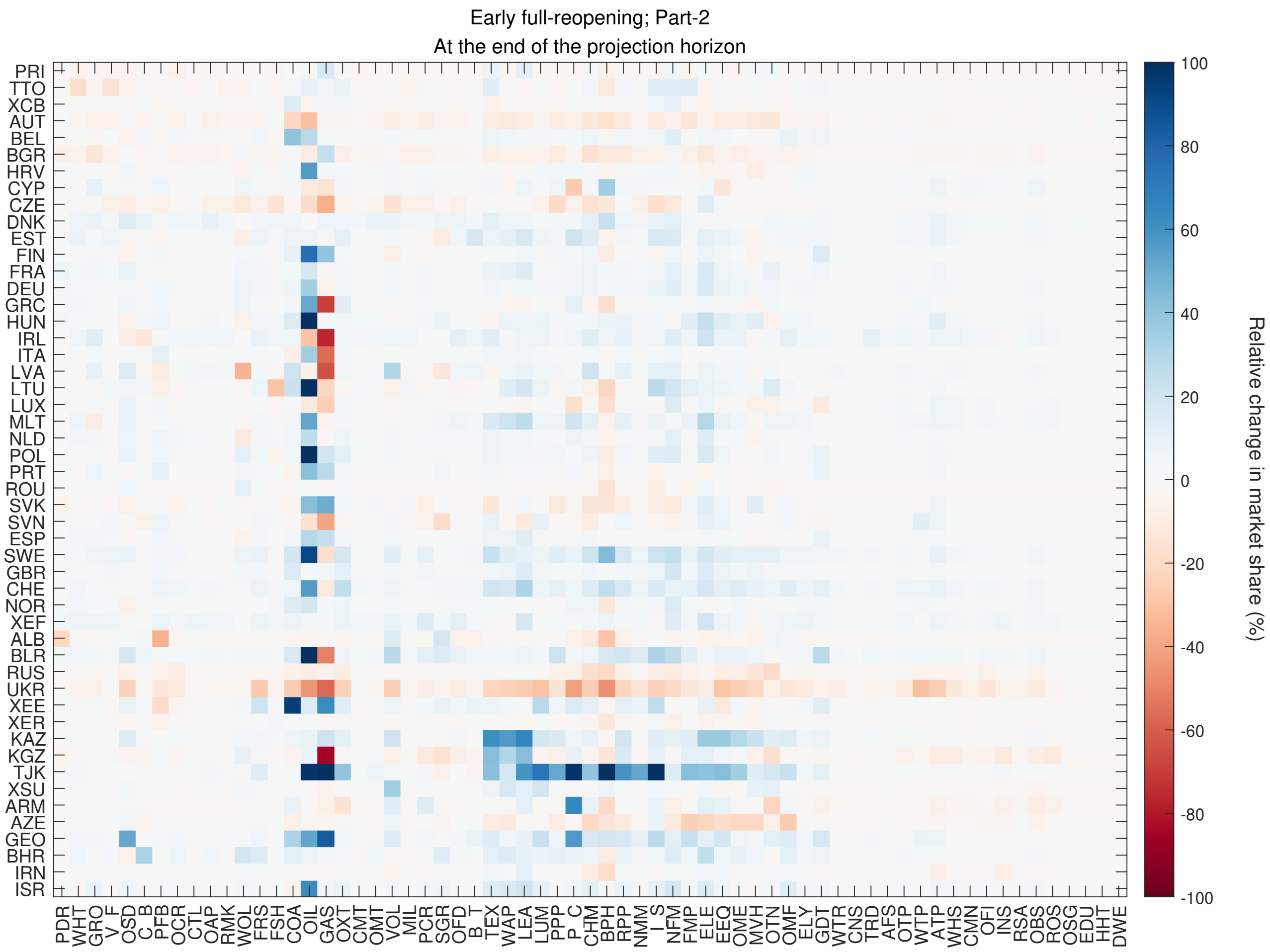

Supplementary Figure 7: Each country/region's changes in market share relative to the pre-pandemic level by sectors at the end of the projection horizon under the early full-reopening scenario. Countries/regions and sectors are presented with three-letter codes. The description of country/region and sector codes can be found in Supplementary tables 6-7.

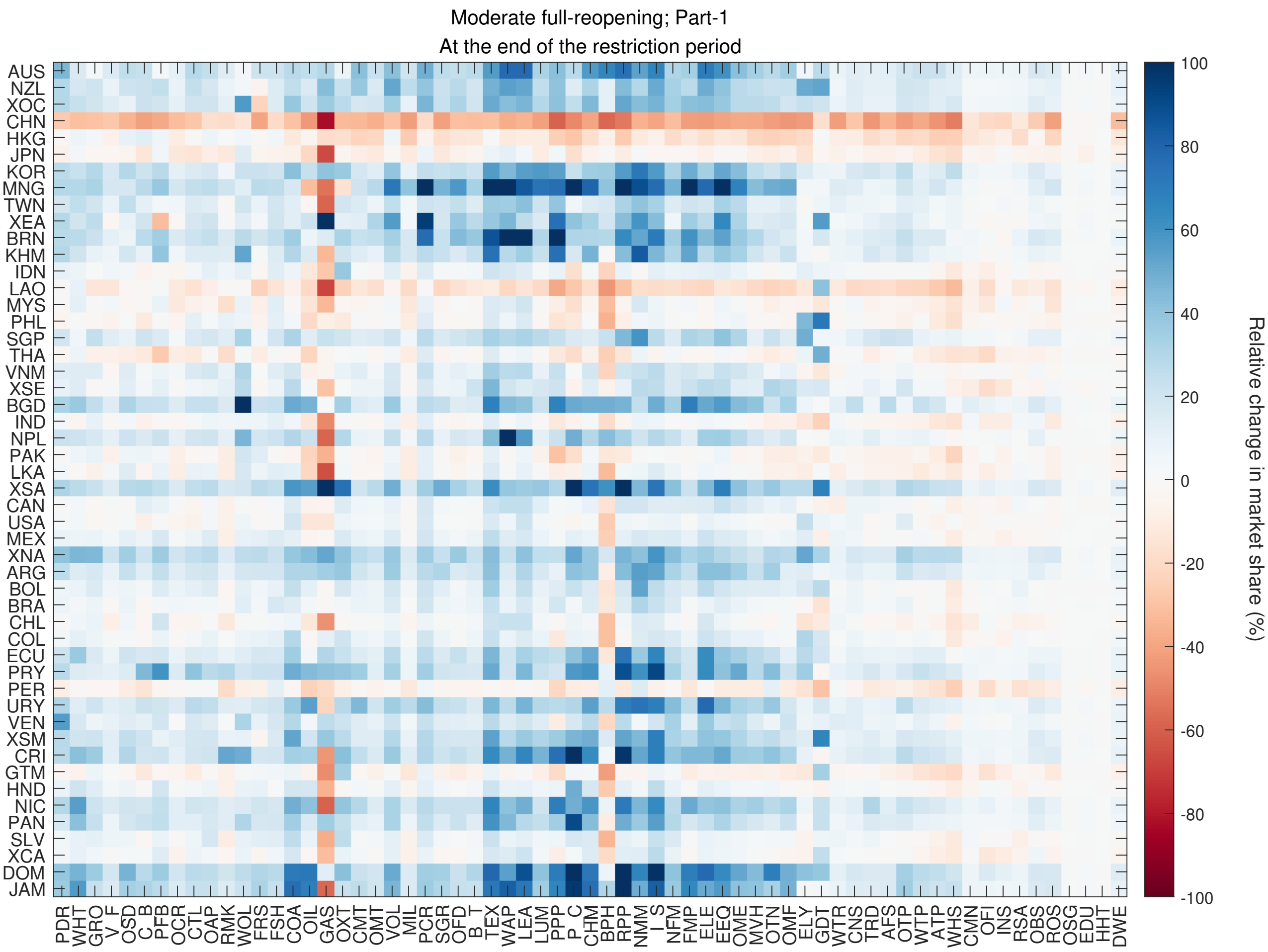

Supplementary Figure 8: Each country/region's changes in market share relative to the pre-pandemic level by sectors at the end of the restriction period under the moderate full-reopening scenario. Countries/regions and sectors are presented with three-letter codes. The description of country/region and sector codes can be found in Supplementary tables 6-7.

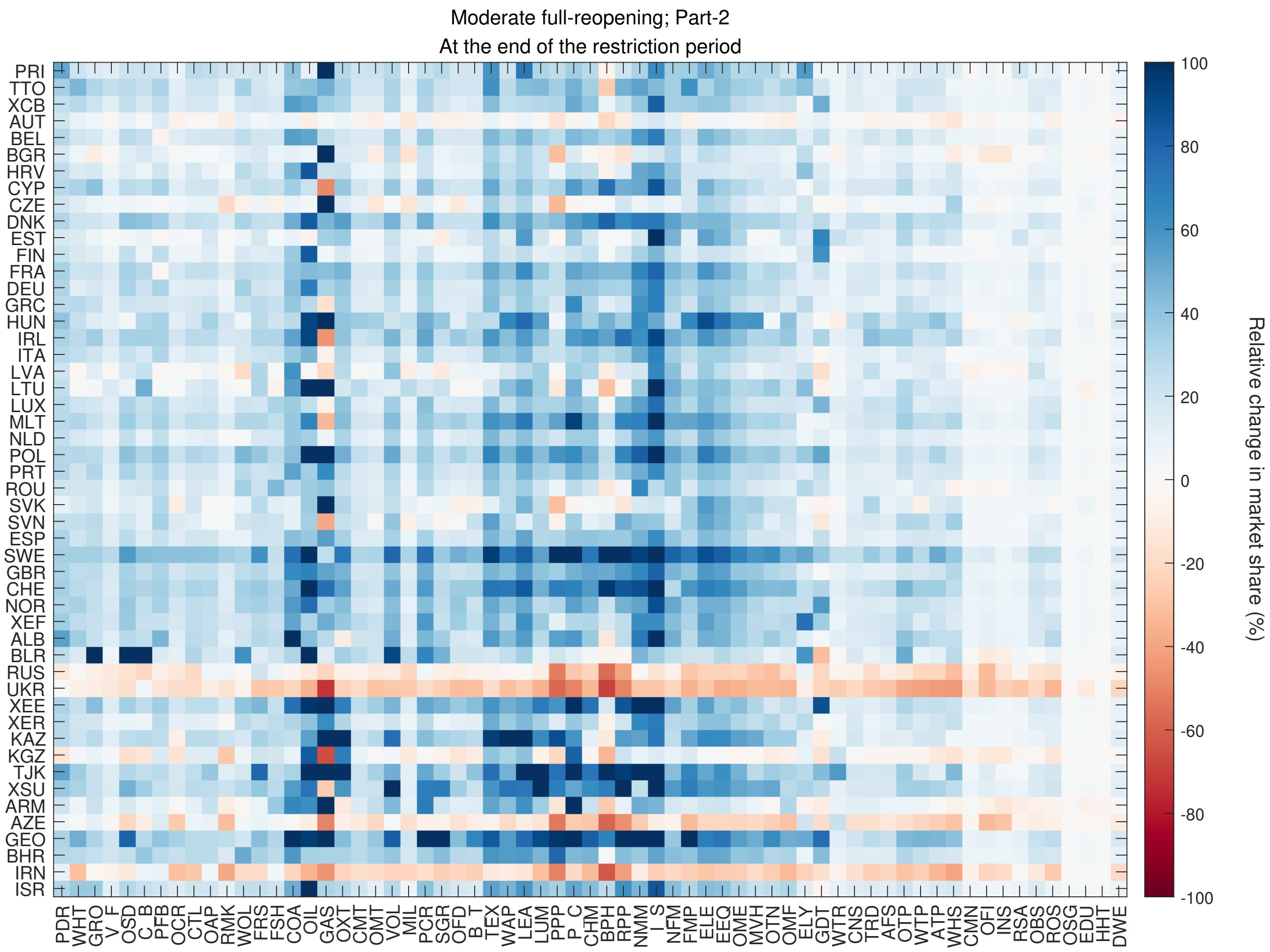

Supplementary Figure 9: Each country/region's changes in market share relative to the pre-pandemic level by sectors at the end of the restriction period under the moderate full-reopening scenario. Countries/regions and sectors are presented with three-letter codes. The description of country/region and sector codes can be found in Supplementary tables 6-7.

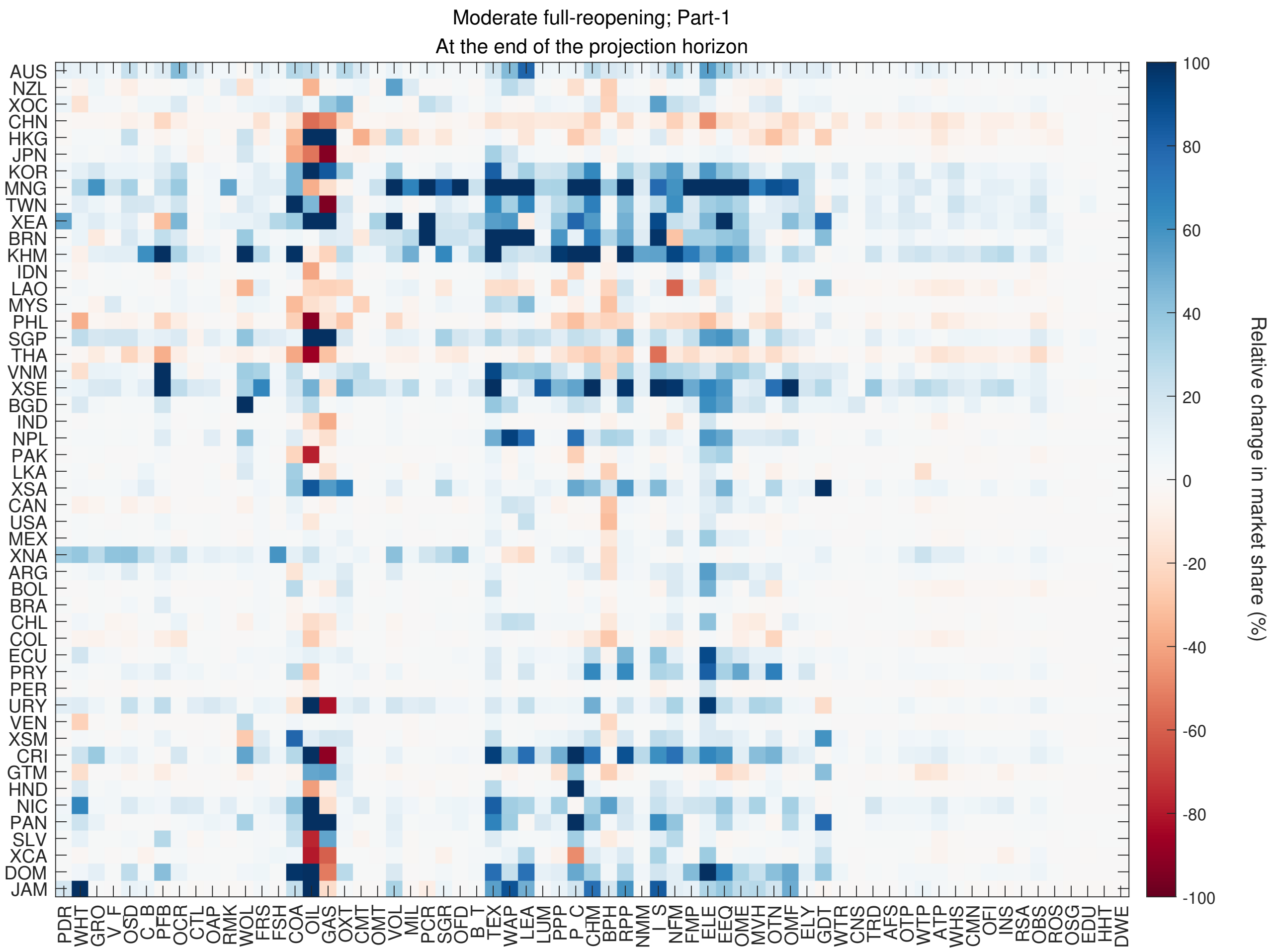

Supplementary Figure 10: Each country/region's changes in market share relative to the pre-pandemic level by sectors at the end of the projection horizon under the moderate full-reopening scenario. Countries/regions and sectors are presented with three-letter codes. The description of country/region and sector codes can be found in Supplementary tables 6-7.

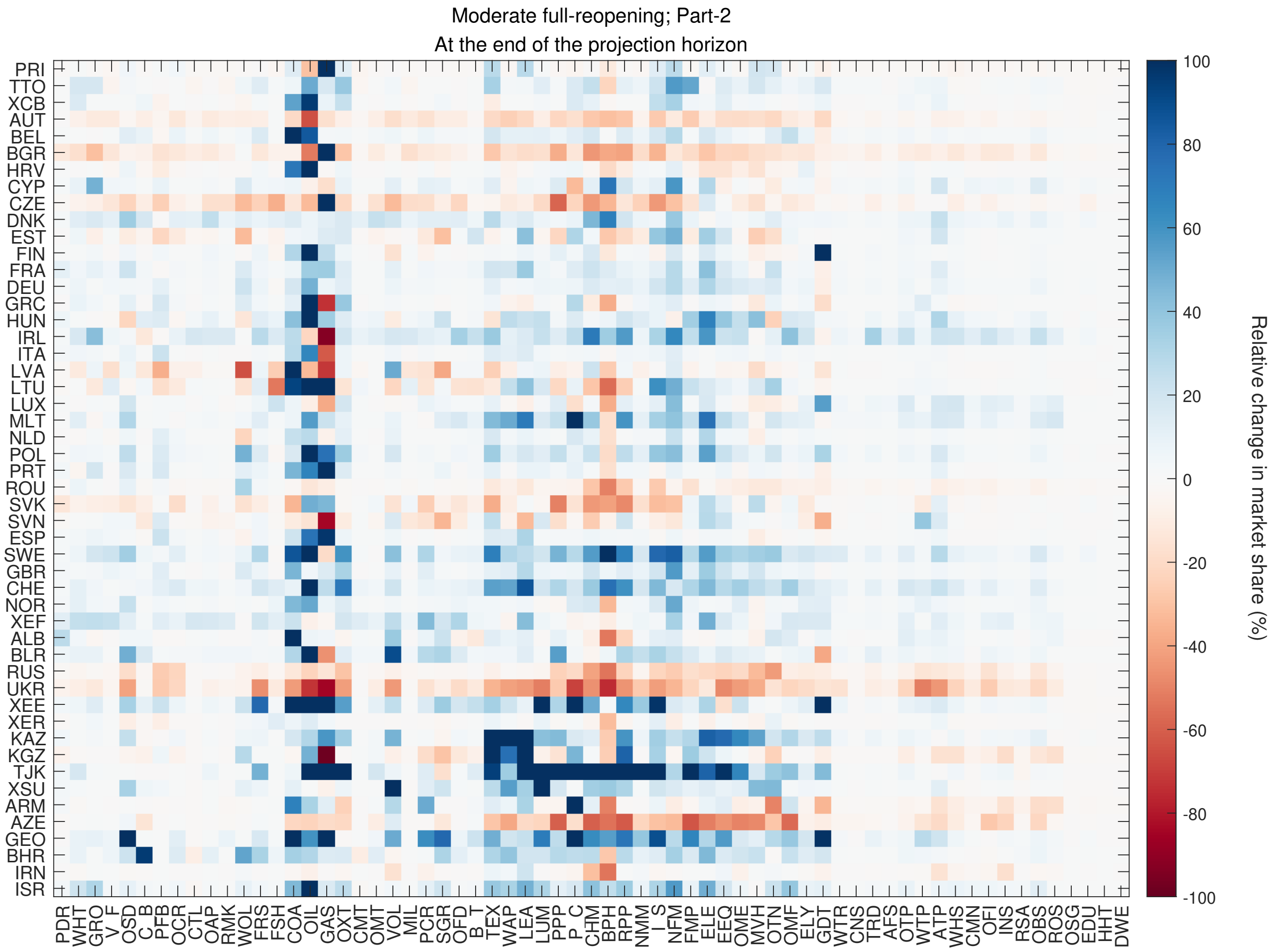

Supplementary Figure 11: Each country/region's changes in market share relative to the pre-pandemic level by sectors at the end of the projection horizon under the late full-reopening scenario. Countries/regions and sectors are presented with three-letter codes. The description of country/region and sector codes can be found in Supplementary tables 6-7.

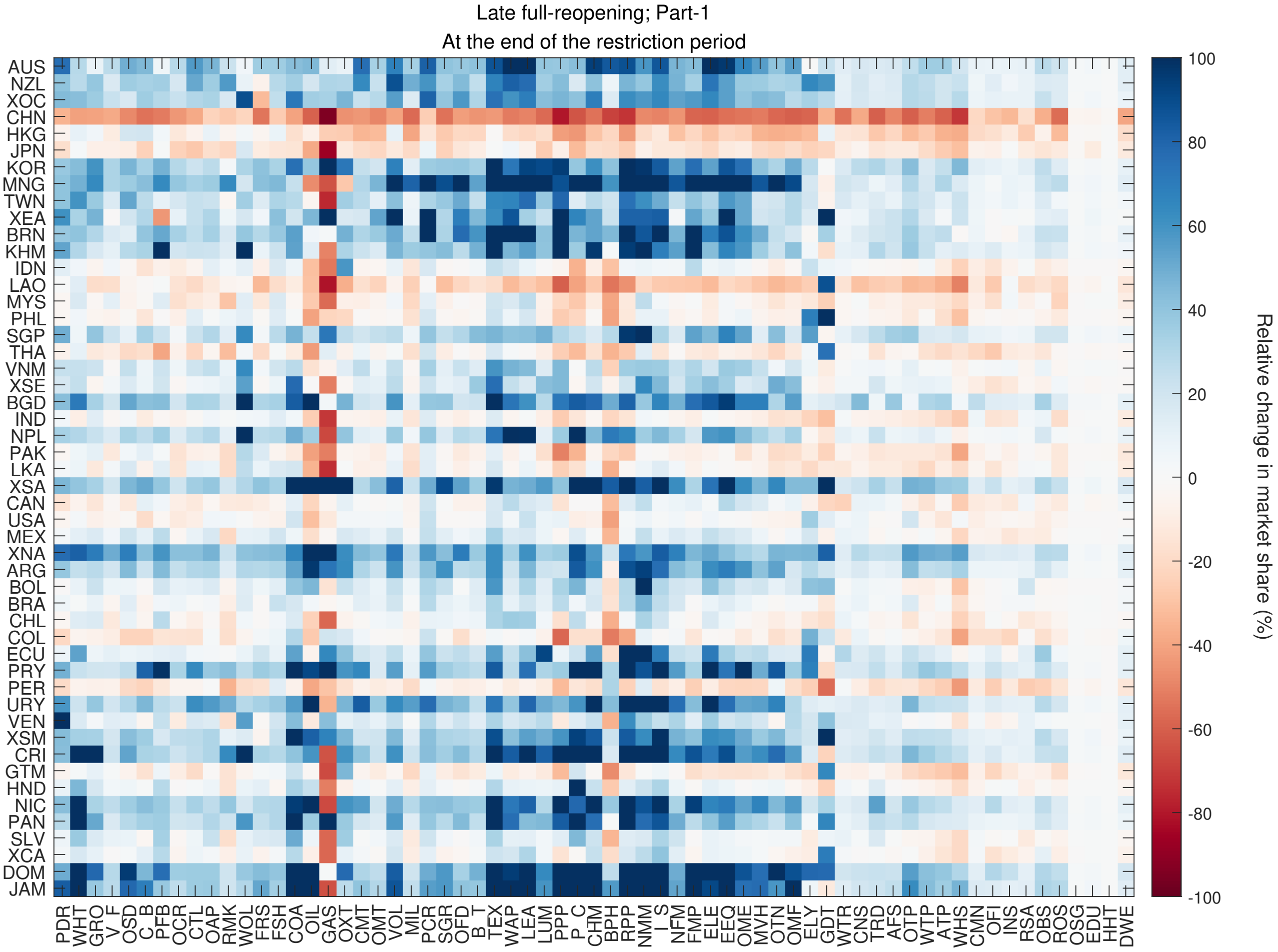

Supplementary Figure 12: Each country/region's changes in market share relative to the pre-pandemic level by sectors at the end of the restriction period under the late full-reopening scenario. Countries/regions and sectors are presented with three-letter codes. The description of country/region and sector codes can be found in Supplementary tables 6-7.

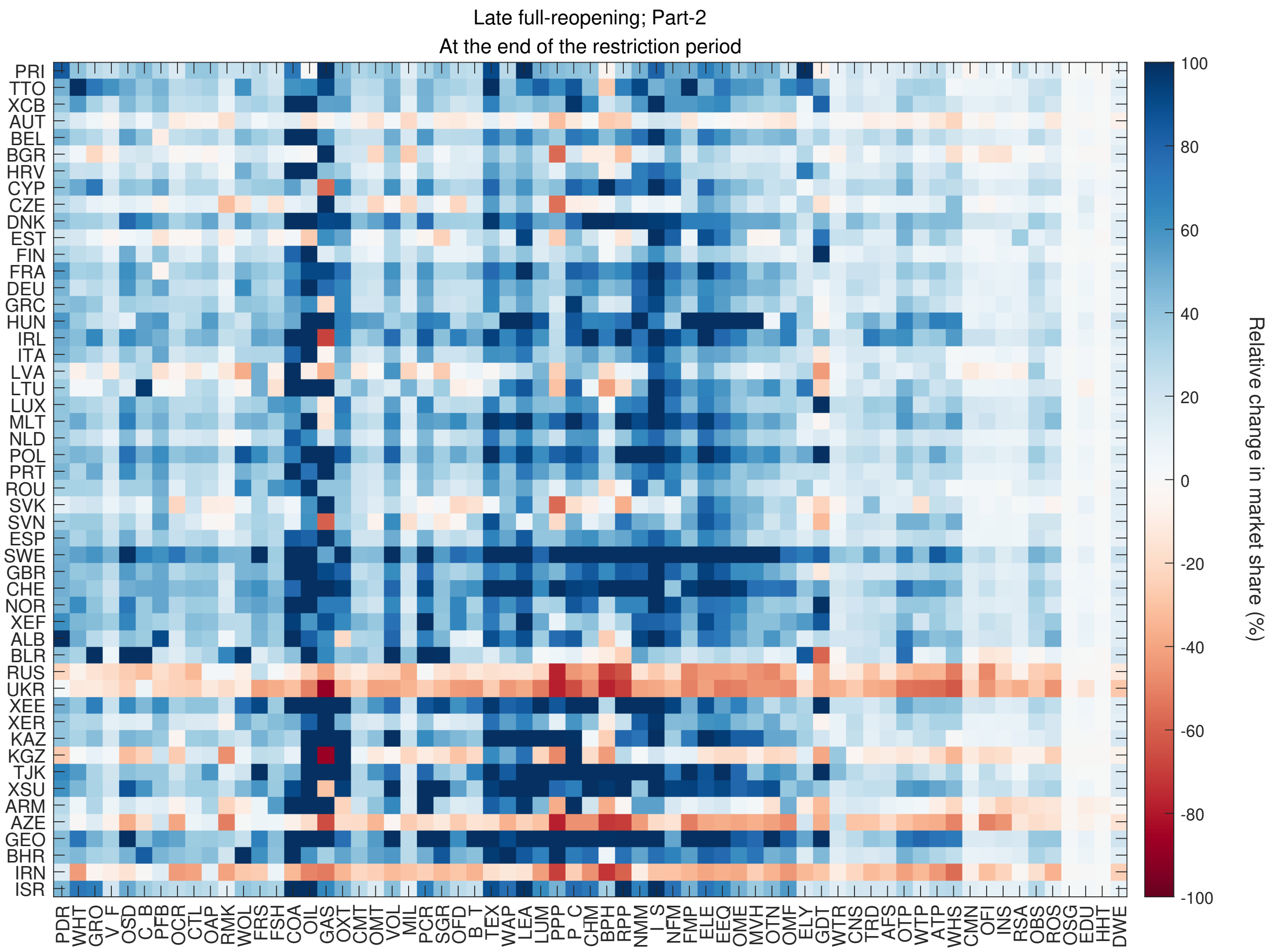

Supplementary Figure 13: Each country/region's changes in market share relative to the pre-pandemic level by sectors at the end of the restriction period under the late full-reopening scenario. Countries/regions and sectors are presented with three-letter codes. The description of country/region and sector codes can be found in Supplementary tables 6-7.

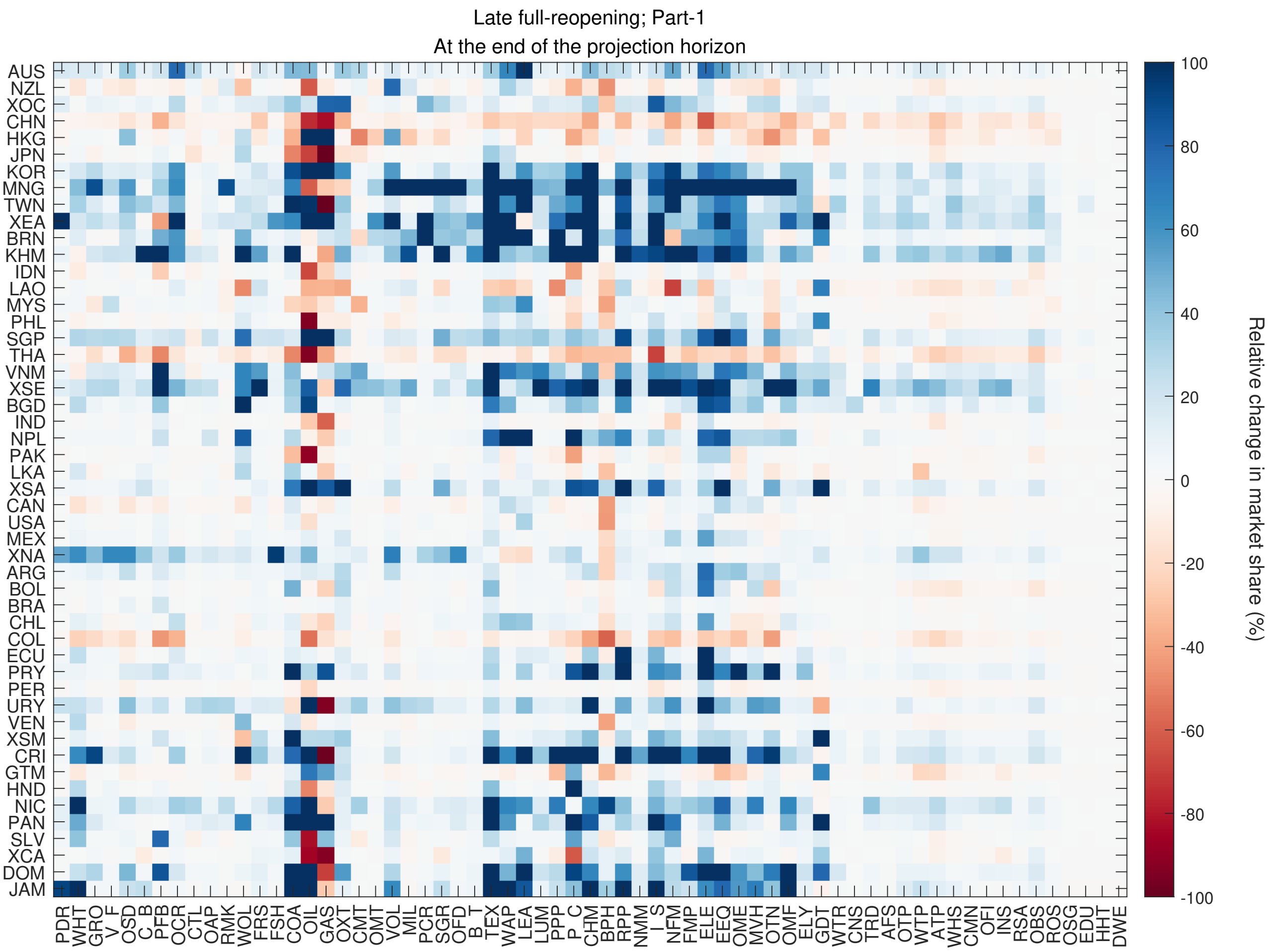

Supplementary Figure 14: Each country/region's changes in market share relative to the pre-pandemic level by sectors at the end of the projection horizon under the late full-reopening scenario. Countries/regions and sectors are presented with three-letter codes. The description of country/region and sector codes can be found in Supplementary tables 6-7.

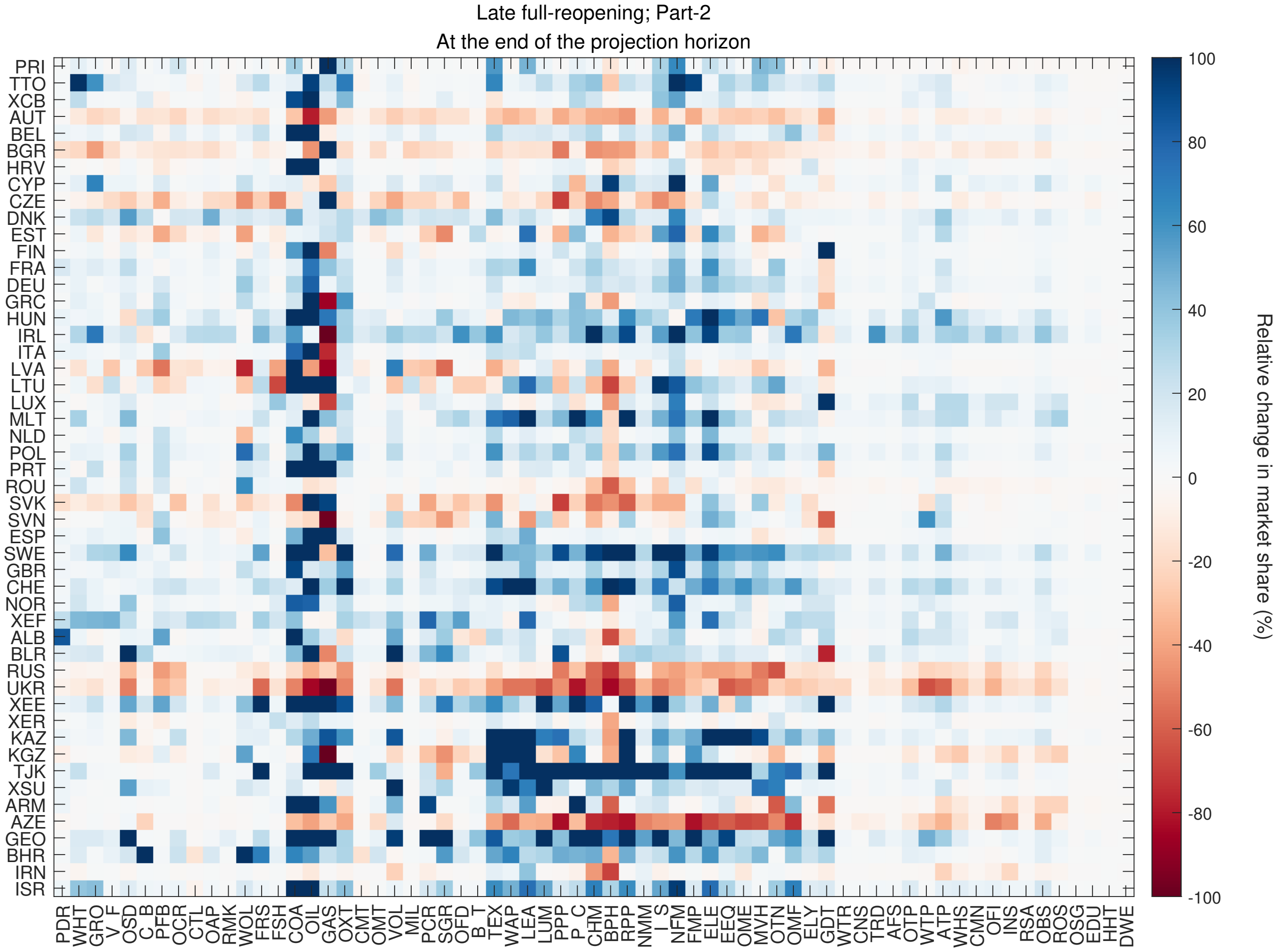

Supplementary Figure 15: Each country/region's changes in market share relative to the pre-pandemic level by sectors at the end of the projection horizon under the moderate full-reopening scenario. Countries/regions and sectors are presented with three-letter codes. The description of country/region and sector codes can be found in Supplementary tables 6-7.

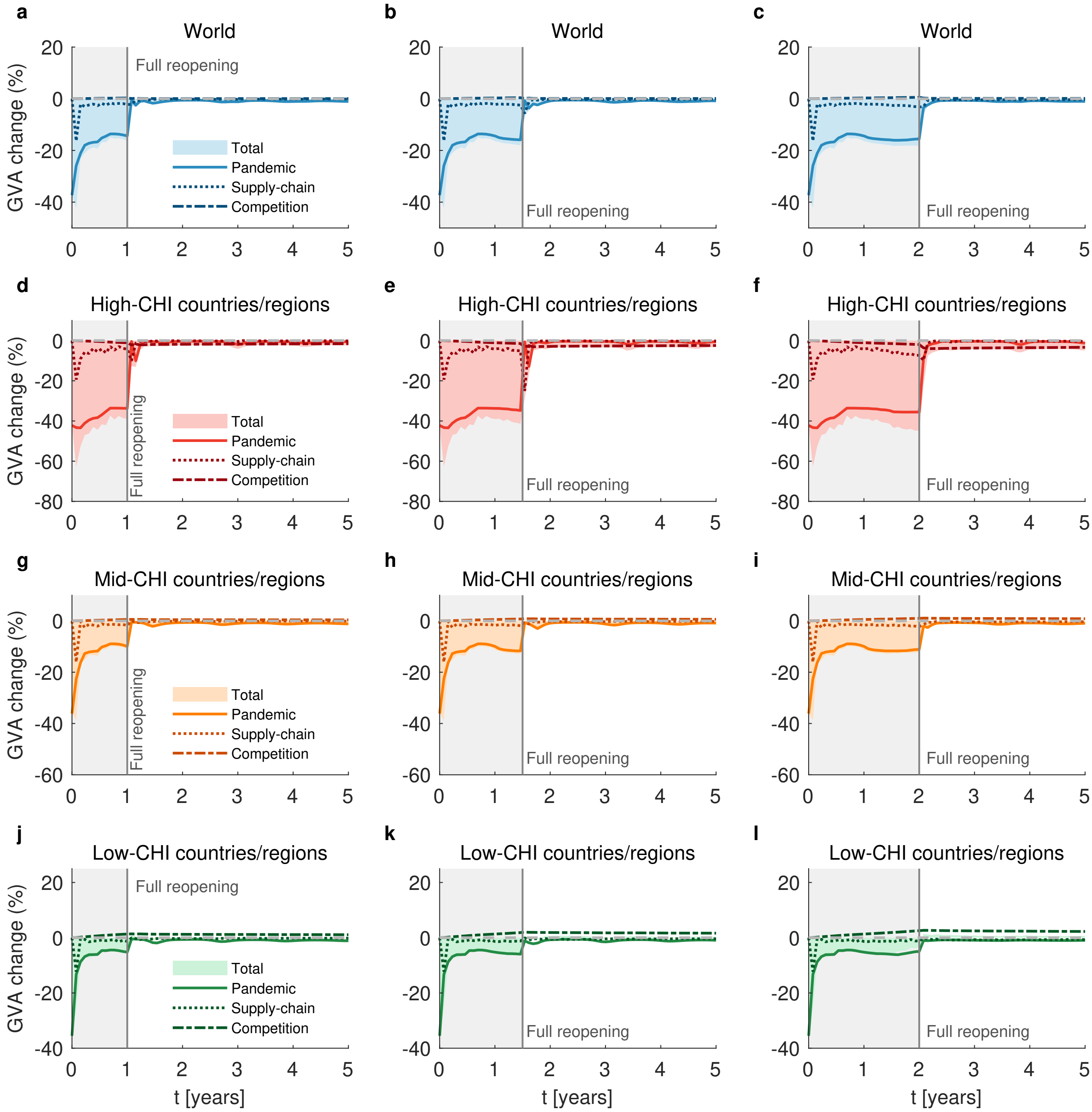

Supplementary Figure 16: Supply-chain impacts of different global reopening scenarios. **a-l**, The total, pandemic-induced, supply disruption-induced, and competition-induced gross value added (GVA) change relative to pre-pandemic levels in all (blue; **a-c**), high-CHI (red; **d-f**), mid-CHI (orange; **g-i**), and low-CHI (green; **j-l**) countries/regions under different global reopening scenarios. The left, middle, and right panels correspond to the results under the early, moderate, and late full-reopening scenarios, respectively. The grey area and the solid grey line indicate the restriction period and the end of the restriction period. The grey dashed line indicates the pre-pandemic level. The total, pandemic-induced, supply-chain disruption-induced, and competition-induced GVA change are represented by shaded areas, solid, dotted, and dash-dotted lines, respectively. $\rho = 0.002$. Other parameters are the same as in the main text.

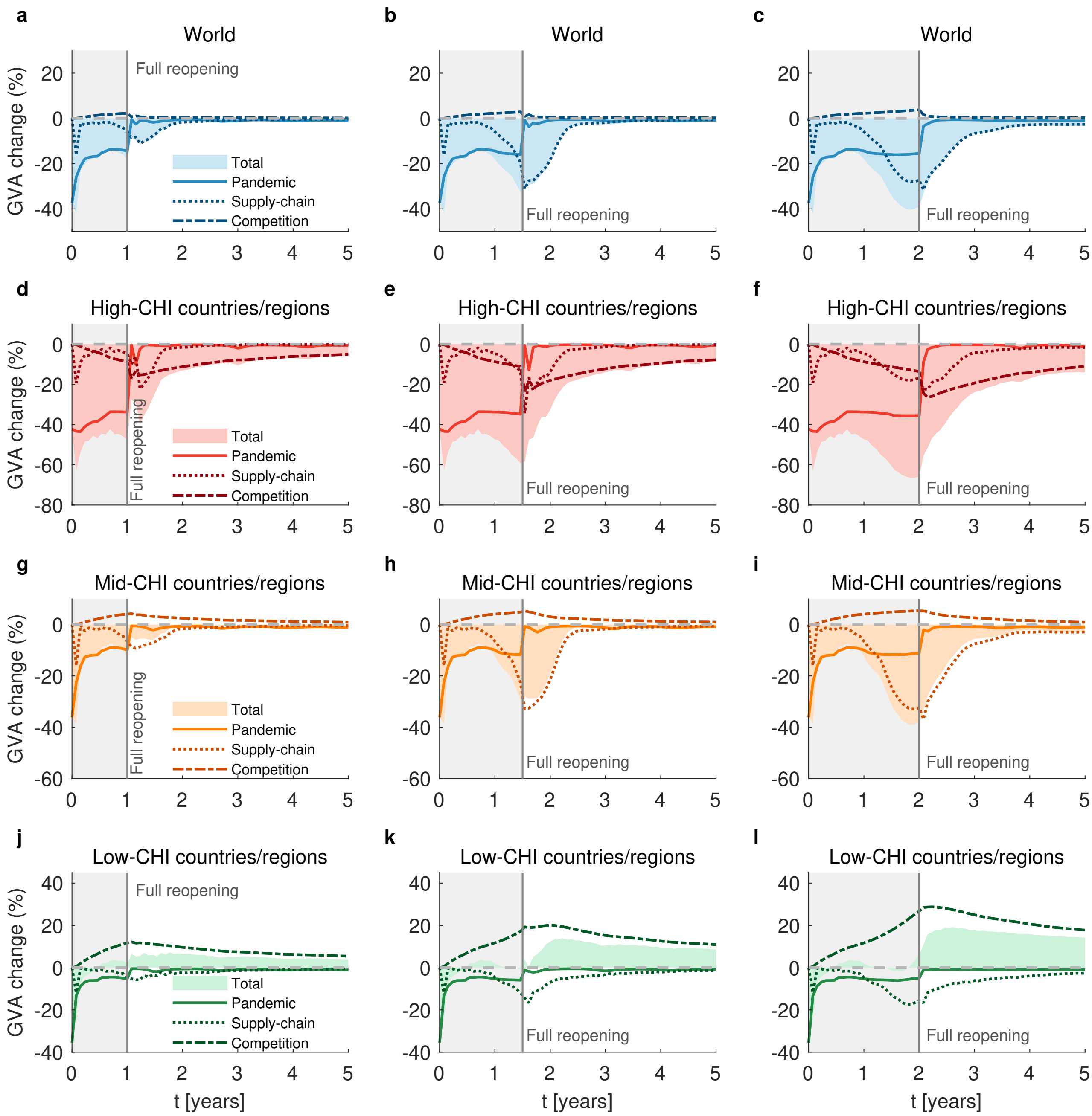

Supplementary Figure 17: Supply-chain impacts of different global reopening scenarios. **a-l**, The total, pandemic-induced, supply disruption-induced, and competition-induced gross value added (GVA) change relative to pre-pandemic levels in all (blue; **a-c**), high-CHI (red; **d-f**), mid-CHI (orange; **g-i**), and low-CHI (green; **j-l**) countries/regions under different global reopening scenarios. The left, middle, and right panels correspond to the results under the early, moderate, and late full-reopening scenarios, respectively. The grey area and the solid grey line indicate the restriction period and the end of the restriction period. The grey dashed line indicates the pre-pandemic level. The total, pandemic-induced, supply-chain disruption-induced, and competition-induced GVA change are represented by shaded areas, solid, dotted, and dash-dotted lines, respectively. $\rho = 0.02$. Other parameters are the same as in the main text.

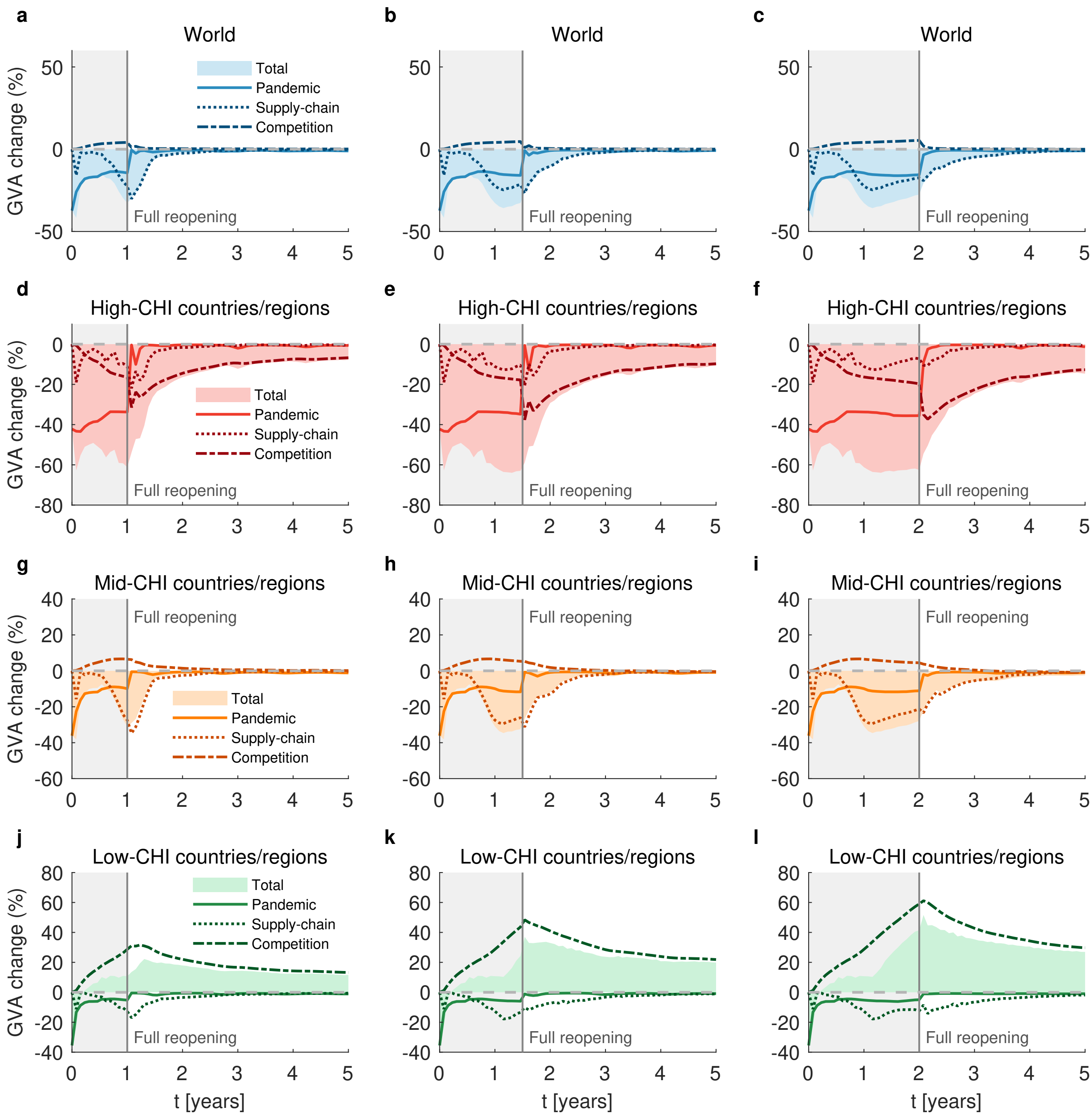

Supplementary Figure 18: Supply-chain impacts of different global reopening scenarios. **a-l**, The total, pandemic-induced, supply disruption-induced, and competition-induced gross value added (GVA) change relative to pre-pandemic levels in all (blue; **a-c**), high-CHI (red; **d-f**), mid-CHI (orange; **g-i**), and low-CHI (green; **j-l**) countries/regions under different global reopening scenarios. The left, middle, and right panels correspond to the results under the early, moderate, and late full-reopening scenarios, respectively. The grey area and the solid grey line indicate the restriction period and the end of the restriction period. The grey dashed line indicates the pre-pandemic level. The total, pandemic-induced, supply-chain disruption-induced, and competition-induced GVA change are represented by shaded areas, solid, dotted, and dash-dotted lines, respectively. $\rho = 0.05$. Other parameters are the same as in the main text.

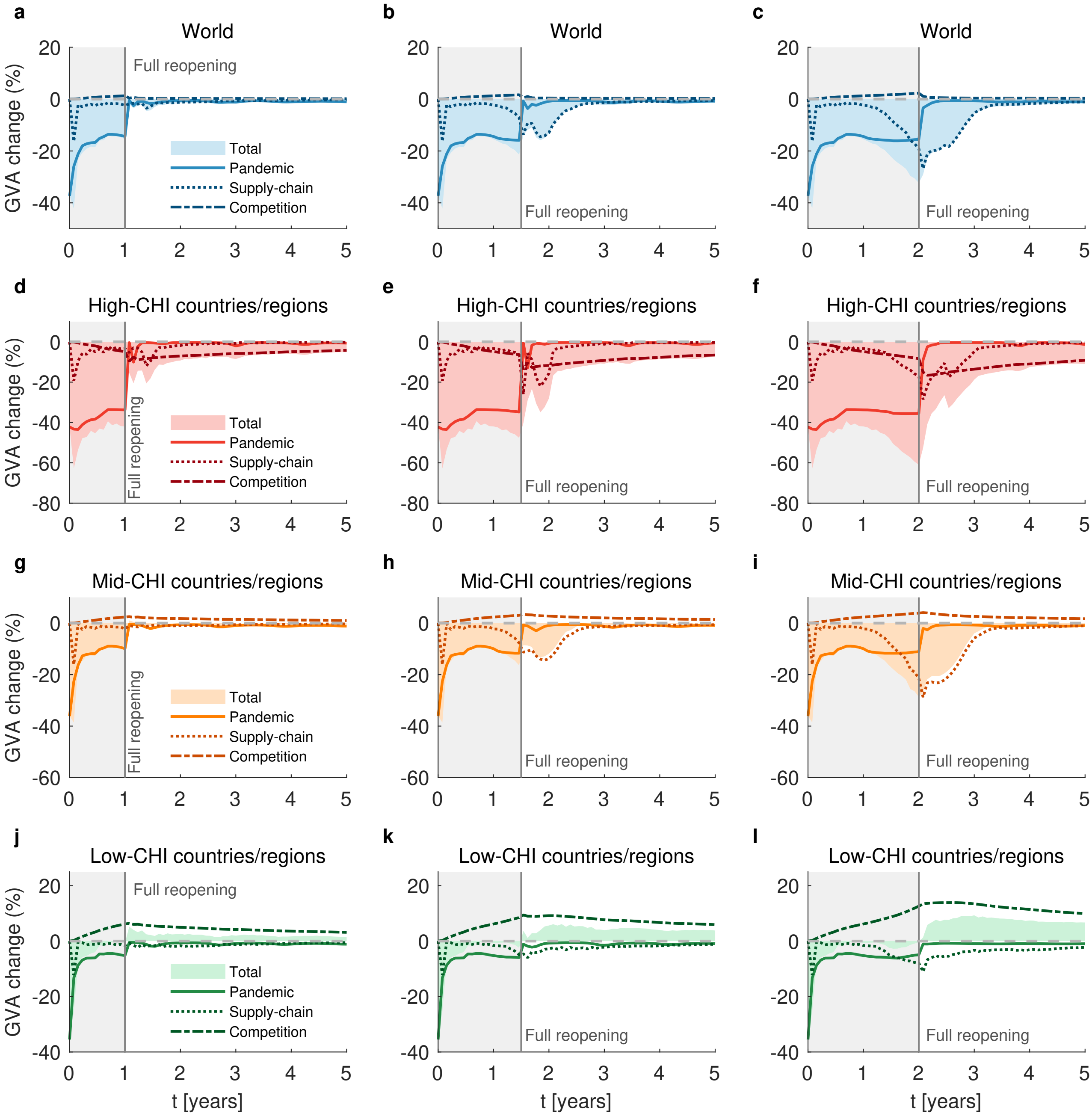

Supplementary Figure 19: Supply-chain impacts of different global reopening scenarios. **a-l**, The total, pandemic-induced, supply disruption-induced, and competition-induced gross value added (GVA) change relative to pre-pandemic levels in all (blue; **a-c**), high-CHI (red; **d-f**), mid-CHI (orange; **g-i**), and low-CHI (green; **j-l**) countries/regions under different global reopening scenarios. The left, middle, and right panels correspond to the results under the early, moderate, and late full-reopening scenarios, respectively. The grey area and the solid grey line indicate the restriction period and the end of the restriction period. The grey dashed line indicates the pre-pandemic level. The total, pandemic-induced, supply-chain disruption-induced, and competition-induced GVA change are represented by shaded areas, solid, dotted, and dash-dotted lines, respectively. $\varphi = 0.3$. Other parameters are the same as in the main text.

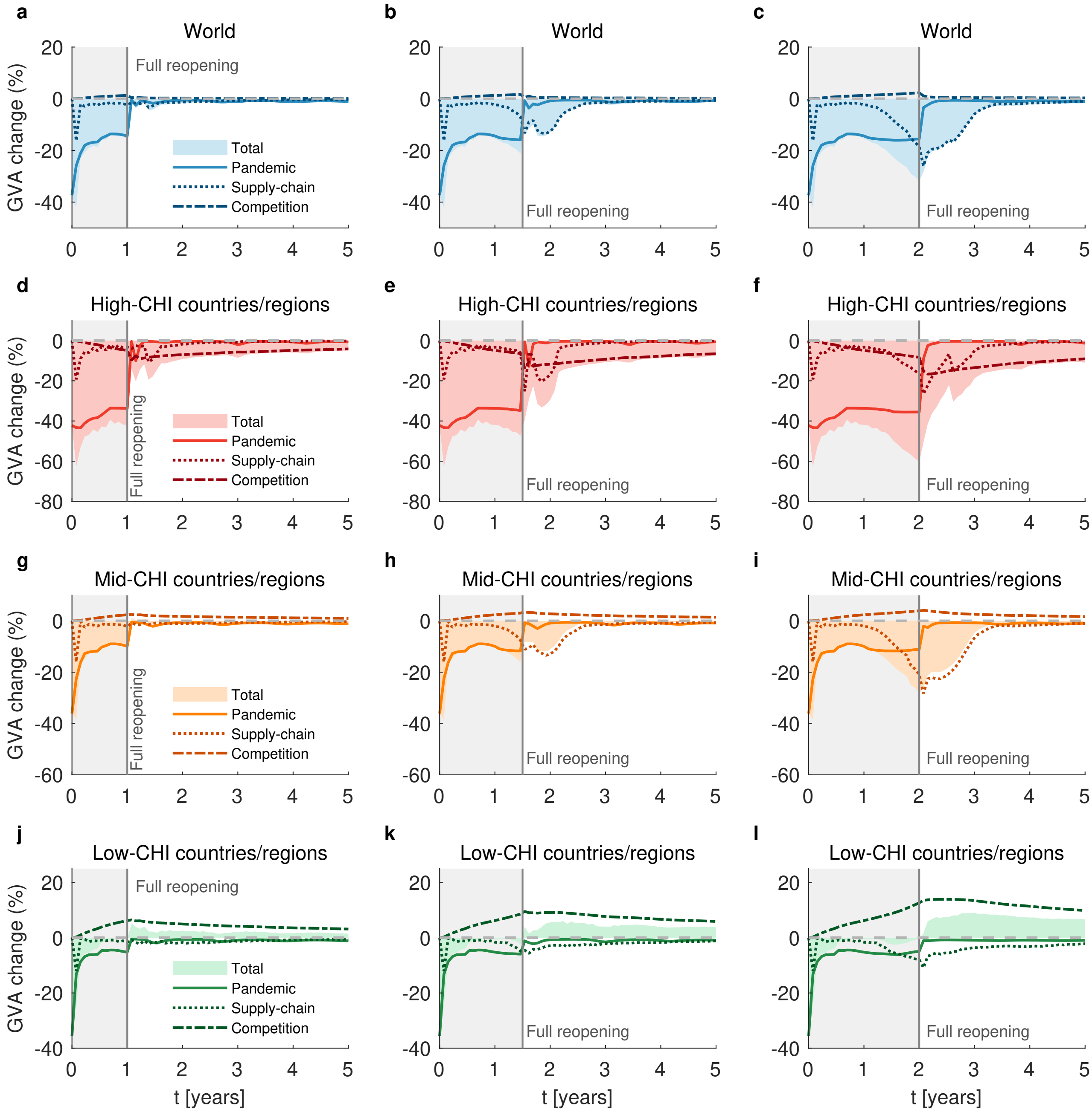

Supplementary Figure 20: Supply-chain impacts of different global reopening scenarios. **a**-**l**, The total, pandemic-induced, supply disruption-induced, and competition-induced gross value added (GVA) change relative to pre-pandemic levels in all (blue; **a**-**c**), high-CHI (red; **d**-**f**), mid-CHI (orange; **g**-**i**), and low-CHI (green; **j**-**l**) countries/regions under different global reopening scenarios. The left, middle, and right panels correspond to the results under the early, moderate, and late full-reopening scenarios, respectively. The grey area and the solid grey line indicate the restriction period and the end of the restriction period. The grey dashed line indicates the pre-pandemic level. The total, pandemic-induced, supply-chain disruption-induced, and competition-induced GVA change are represented by shaded areas, solid, dotted, and dash-dotted lines, respectively. $\varphi = 0.9$. Other parameters are the same as in the main text.

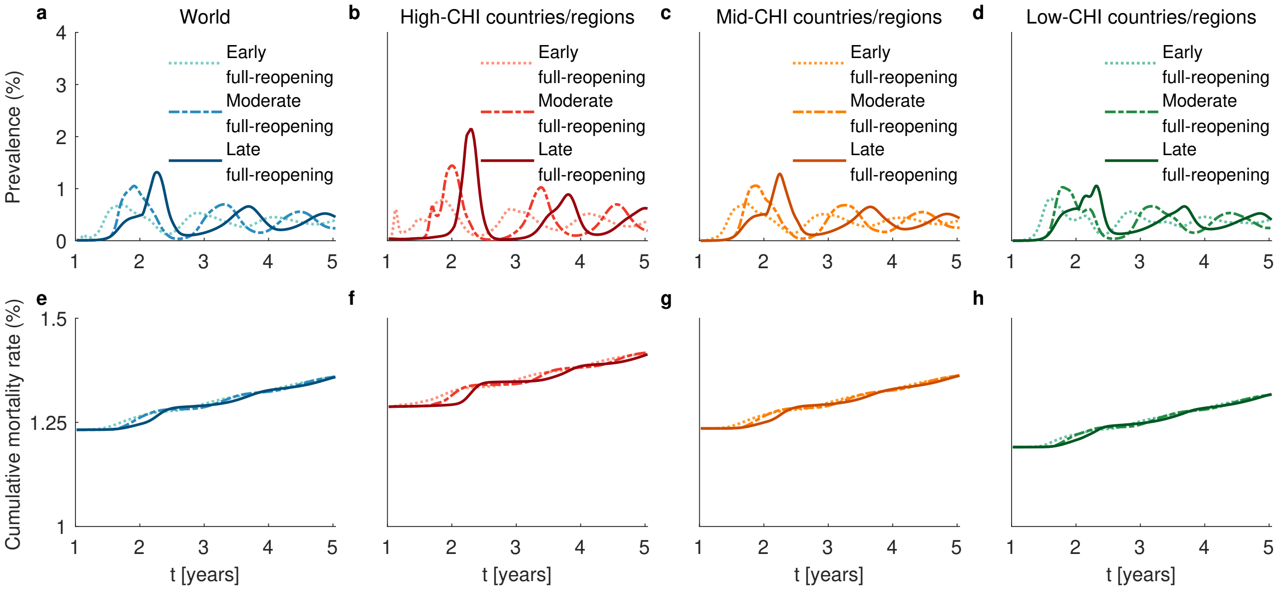

Supplementary Figure 21: Public health impacts of different global reopening scenarios. **a-h**, Time series of the average prevalence (**a-d**) and cumulative mortality rate (**e-h**) in all (**a, e**), high-CHI (**b, f**), mid-CHI (**c, g**), and low-CHI (**d, h**) countries/regions under different global reopening scenarios. Dotted, dash-dotted, and solid lines correspond to the results under the early, moderate, and late full-reopening scenarios. Other parameters are the same as in the main text.

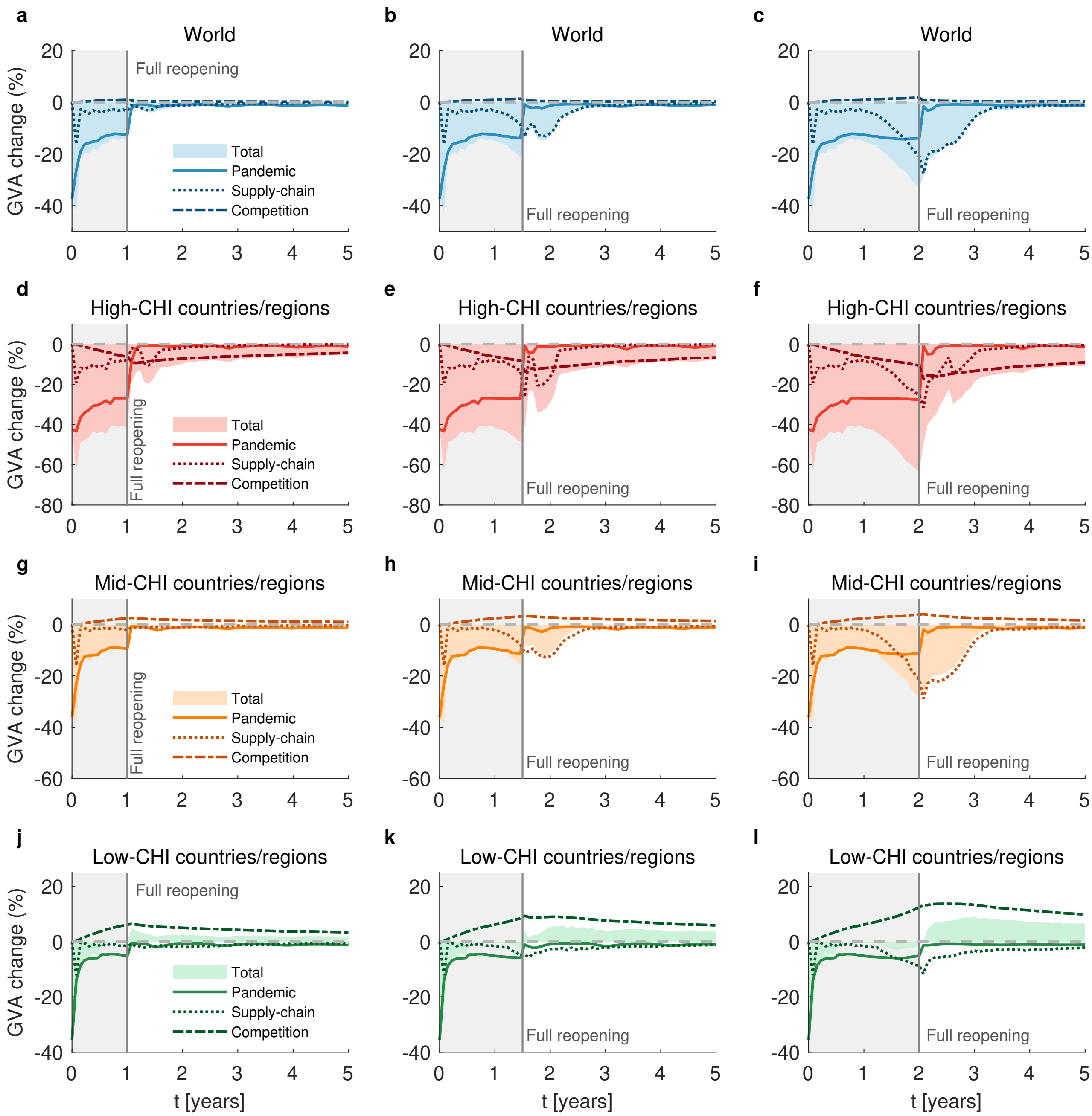

Supplementary Figure 22: Supply-chain impacts of different global reopening scenarios. **a-l**, The total, pandemic-induced, supply disruption-induced, and competition-induced gross value added (GVA) change relative to pre-pandemic levels in all (blue; **a-c**), high-CHI (red; **d-f**), mid-CHI (orange; **g-i**), and low-CHI (green; **j-l**) countries/regions under different global reopening scenarios. The left, middle, and right panels correspond to the results under the early, moderate, and late full-reopening scenarios, respectively. The grey area and the solid grey line indicate the restriction period and the end of the restriction period. The grey dashed line indicates the pre-pandemic level. The total, pandemic-induced, supply-chain disruption-induced, and competition-induced GVA change are represented by shaded areas, solid, dotted, and dash-dotted lines, respectively. $\phi = 0.005$. Other parameters are the same as in the main text.

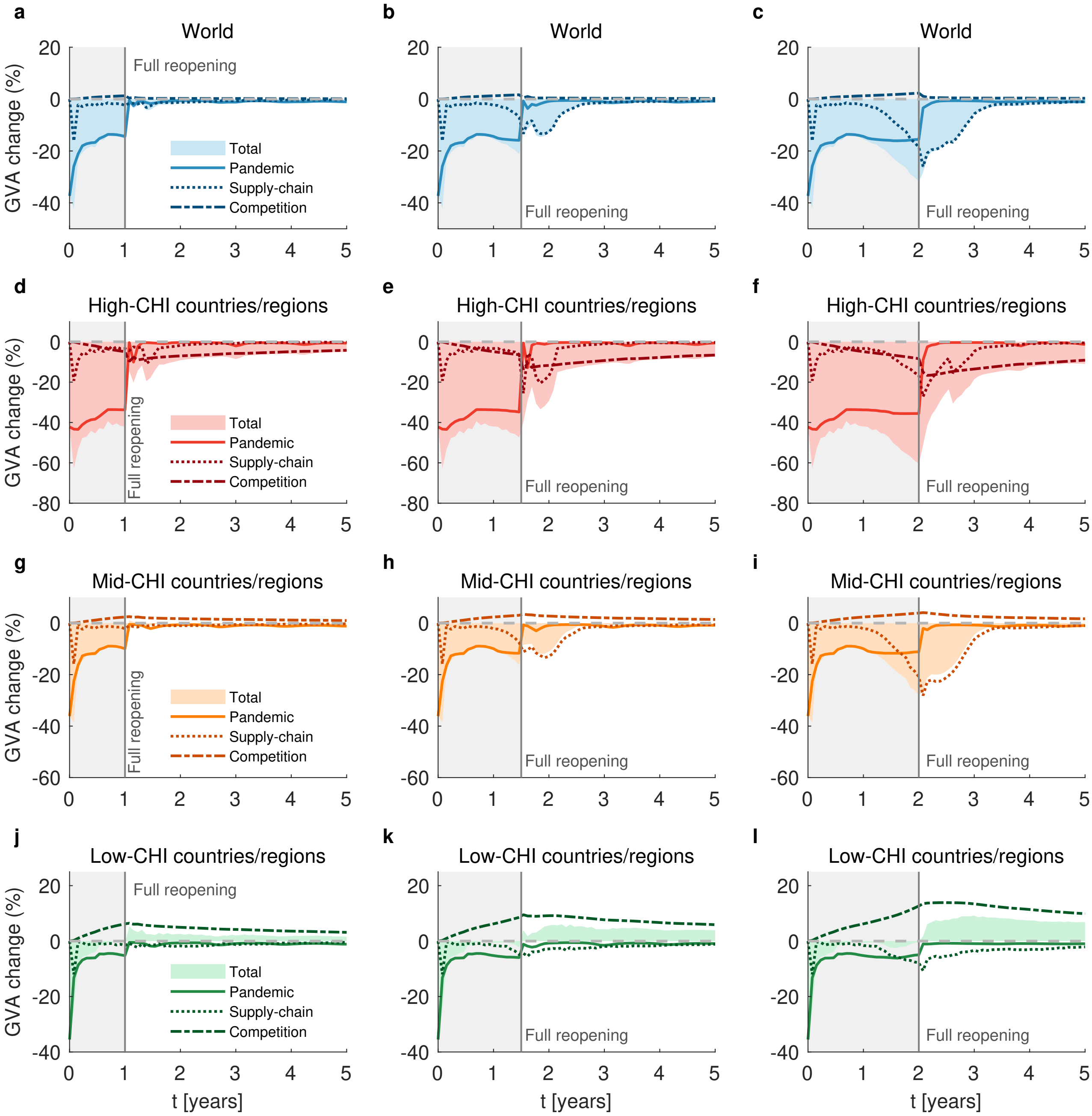

Supplementary Figure 23: Supply-chain impacts of different global reopening scenarios. **a-l**, The total, pandemic-induced, supply disruption-induced, and competition-induced gross value added (GVA) change relative to pre-pandemic levels in all (blue; **a-c**), high-CHI (red; **d-f**), mid-CHI (orange; **g-i**), and low-CHI (green; **j-l**) countries/regions under different global reopening scenarios. The left, middle, and right panels correspond to the results under the early, moderate, and late full-reopening scenarios, respectively. The grey area and the solid grey line indicate the restriction period and the end of the restriction period. The grey dashed line indicates the pre-pandemic level. The total, pandemic-induced, supply-chain disruption-induced, and competition-induced GVA change are represented by shaded areas, solid, dotted, and dash-dotted lines, respectively. $I_{thre} = 0.1$. Other parameters are the same as in the main text.

Supplementary Table 4: Model parameter symbols part 1

Denotation	Definition	Values	References
N_i	Population size of country i		
S_i	# Susceptible individuals of country i		
V_i	# Vaccinated individuals of country i		
E_i^S	# Exposed individuals without vaccinal immunity of country i		
E_i^V	# Exposed individuals with vaccinal immunity of country i		
I_i^S	# Infectious individuals without vaccinal immunity of country i		
I_i^V	# Infectious individuals with vaccinal immunity of country i		
R_i	# Recovered individuals of country i		
D_i	# Deceased individuals of country i		
c_i	The effectiveness of NPIs		
$c_i^{stringent}$	The effectiveness of the most stringent NPIs		
c_i^{mild}	The effectiveness of the mildest NPIs		
β	The transmission rate	10/5.6	[7]
η	The efficacy of vaccines against infection	0.75	[8]
ϵ	The efficacy of vaccines against death	0.98	[9]
$R_{e,i}$	The local effective reproduction number		
k	Shape parameter in calculating $R_{e,i}$		
Λ_i^S	The transition rate from S_i to E_i^S		
Λ_i^V	The transition rate from V_i to E_i^V		
ϕ_i	Vaccination rate		
$1/\varepsilon$	Duration of vaccinal immunity	7 months	[10]
$1/\sigma$	The incubation period	1.2 days	[2]
$1/\alpha$	The infectious period	5.6 days	[2]
ν	Severity of the virus (infection fatality rate)	0.03	[2]
$1/\psi$	Duration of natural immunity	900 days	[2]
υ	The natural mortality rate	7.7/1000 yr^{-1}	[11]
ζ_i	The natural birth rate		
$\hat{\gamma}_i$	Reduction in the number of international travelers for country i before reopening		
G_{ij}	The number of individuals travelling between country i and country j		
$\overline{G}_{ij}$	The number of individuals travelling between country i and country j before the pandemic		[3]
$CHI_i(t)$	The CHI score of country i at time t		[1]
CHI_{CHN}	The CHI score of China on April 15, 2022	79.17	[1]
$c_{CHN}^{stringent}$	The effectiveness of the most stringent NPIs adopted by China on April 15, 2022	0.8	[2]
c_{CHN}^{mild}	The effectiveness of the mildest NPIs adopted by China on April 15, 2022	0.6	[2]
$\hat{\gamma}_{CHN}$	Reduction in the number of international travelers for China in 2020 compared to that in 2019	0.8	[3]

Supplementary Table 5: Model parameter symbols part 2

Denotation	Definition
L_{ai}^{*}	Labour input for firm ai before the pandemic
x_{ai}^{*}	The output of firm ai before the pandemic
$Z_{bj\to ai}^{*}$	The trade flow from firm bj to firm ai before the pandemic
$y_{bj\to i}^{*}$	The trade flow from firm bj to the household in country i before the pandemic
$DemH_{i}^{a^*}$	The demand of product a for the household in country i before the pandemic
q_{ai}^{L}	The input coefficients
q_{ai}^{b}	The input coefficients
ϑ_{a}^{P}	The effects of COVID-19 restrictions on labour availability for sector a
ϑ_{a}^{D}	The utmost demand change of product a for household during the pandemic
$\mathcal{P}_{ai}$	The set of intermediate products for firm ai
$L_{ai}(t)$	Labour input for firm ai at time t
$\kappa_{ai}(t)$	The production extension ratio for firm ai at time t
$r_{ai}(t)$	The fraction of workers who are unable to work for firm ai at time t
$Inv_{ai}^{b}(t)$	The inventory of intermediate product b that firm ai holds at then end of time t
$PTF_{bj\to ai}(t)$	The amount of product b arrived at firm ai from firm bj at time t
$PTH_{bj\to i}(t)$	The amount of product b arrived at the household in country i from firm bj at time t
$x_{ai}^{A}(t)$	The actual output of firm ai at time t
$x_{ai}^{MAX}(t)$	The maximum output of firm ai at time t
$\hat{x}_{ai}(t)$	The production capacity of firm ai at time t
$OrdH_{j\to ai}(t)$	The orders issued by the household in country j to firm ai at time t
$OrdF_{bj\to ai}(t)$	The orders issued by firm bj to firm ai at time t
$\Theta_{ai}(t)$	The reliability of firm ai at time t
φ	The diminishing factor
$\xi_{ai}(t)$	The profitability of firm ai at time t
$\bar{\xi}_{a}(t)$	The average profitability in sector a at time t
$M_{ai}(t)$	The market share of firm ai at time t
$TarInv_{ai}^{b}(t)$	The target inventory of intermediate product b for firm ai at time t
n_{ai}	The number of time steps of intermediate consumption in demand for firm ai
$DemF_{ai}^{b}(t)$	The demand of intermediate product b for firm ai at time t
$DemH_{i}^{a}(t)$	The demand of product a for the household in country i at time t
I_{thre}	The threshold of prevalence
ρ	The rate of evolutionary change

Supplementary Table 6: GTAP sector classification and multiplier

Sector Code	Sector Name	ϑ_{a}^{P} [12]	ϑ_{a}^{D} [13]
pdr	Rice	0.5	1
wht	Wheat	0.5	1
gro	Other Grains	0.5	1
v_f	Veg & Fruit	0.5	1
osd	Oil Seeds	0.5	1
c_b	Cane & Beet	0.5	1
pfb	Fibres crops	0.5	1
ocr	Other Crops	0.5	1
ctl	Cattle	0.5	1
oap	Other Animal Products	0.5	1
rmk	Raw milk	0.5	1

wol	Wool	0.5	1
frs	Forestry	0.5	1
fsh	Fishing	0.5	1
coa	Coal	1	1
oil	Oil	1	1
gas	Gas	1	1
oxt	Other Mining Extraction	1	1
cmt	Cattle Meat	1	1
omt	Other Meat	1	1
vol	Vegetable Oils	1	1
mil	Milk	1	1
pcr	Processed Rice	1	1
sgr	Sugar and molasses	1	1
ofd	Other Food	1	1
b_t	Beverages and Tobacco products	1	1
tex	Manufacture of textiles	1	0.5
wap	Manufacture of wearing apparel	1	0.5
lea	Manufacture of leather and related products	1	0.5
lum	Lumber	1	0.9
ppp	Paper & Paper Products	1	0.9
p_c	Petroleum & Coke	1	0.75
chm	Manufacture of chemicals and chemical products	1	0.9
bph	Manufacture of pharmaceuticals, medicinal chemical and botanical products	1	0.9
rpp	Manufacture of rubber and plastics products	1	0.9
nmm	Manufacture of other non-metallic mineral products	1	0.9
i_s	Iron & Steel	1	0.9
nfm	Non-Ferrous Metals	1	0.9
fmp	Manufacture of fabricated metal products, except machinery and equipment	1	0.9
ele	Manufacture of computer, electronic and optical products	1	1
eeq	Manufacture of electrical equipment	1	0.9
ome	Manufacture of machinery and equipment n.e.c.	1	0.9
mvh	Manufacture of motor vehicles, trailers and semi-trailers	1	0.7
otn	Manufacture of other transport equipment	1	0.7
omf	Other Manufacturing: includes furniture	1	0.9
ely	Electricity; steam and air conditioning supply	0.1	1
gdt	Gas manufacture, distribution	0.1	1
wtr	Water supply; sewerage, waste management and remediation activities	0.1	1
cns	Construction	1	0.75
trd	Wholesale and retail trade; repair of motor vehicles and motorcycles	1	1.1
afs	Accommodation, Food and service activities	1	0.25
otp	Land transport and transport via pipelines	1	0.8
wtp	Water transport	1	0.8
atp	Air transport	1	0.8
whs	Warehousing and support activities	1	0.8
cmn	Information and communication	0.1	0.9
ofi	Other Financial Intermediation	0.1	1
ins	Insurance	0.1	1
rsa	Real estate activities	0.1	0.6
obs	Other Business Services nec	0.1	0.85

ros	Recreation & Other Services	1	0.25
osg	Other Services (Government)	0.1	1.25
edu	Education	0.1	0.85
hht	Human health and social work	0	1
dwe	Dwellings	1	0.75

Supplementary Table 7: Country Alpha 3 ISO codes list

Code	Name	Code	Name
USA	United States	CHN	China
JPN	Japan	DEU	Germany
GBR	United Kingdom	FRA	France
IND	India	BRA	Brazil
ITA	Italy	RUS	Russia

Codes for other countries can be found in
`https://www.iso.org/iso-3166-country-codes.html`

Supplementary References

[1] Thomas Hale, Noam Angrist, Rafael Goldszmidt, Beatriz Kira, Anna Petherick, Toby Phillips, Samuel Webster, Emily Cameron-Blake, Laura Hallas, Saptarshi Majumdar, et al. A global panel database of pandemic policies (oxford covid-19 government response tracker). *Nature Human Behaviour*, 5(4):529–538, 2021.

[2] Jun Cai, Xiaowei Deng, Juan Yang, Kaiyuan Sun, Hengcong Liu, Zhiyuan Chen, Cheng Peng, Xinhua Chen, Qianhui Wu, Junyi Zou, et al. Modeling transmission of sars-cov-2 omicron in china. *Nature Medicine*, pages 1–8, 2022.

[3] OAG. *OAG*, 2020. `https://www.oag.com/`.

[4] Sven Norman Willner, Christian Otto, and Anders Levermann. Global economic response to river floods. *Nature Climate Change*, 8(7):594–598, 2018.

[5] Phillip Bonacich. Factoring and weighting approaches to status scores and clique identification. *Journal of mathematical sociology*, 2(1):113–120, 1972.

[6] Linton C Freeman. A set of measures of centrality based on betweenness. *Sociometry*, pages 35–41, 1977.

[7] Talha Khan Burki. Omicron variant and booster covid-19 vaccines. *The Lancet Respiratory Medicine*, 10(2):e17, 2022.

[8] Carlos Del Rio, Saad B Omer, and Preeti N Malani. Winter of omicron—the evolving covid-19 pandemic. *Jama*, 327(4):319–320, 2022.

[9] Nick Andrews, Julia Stowe, Freja Kirsebom, Samuel Toffa, Ruchira Sachdeva, Charlotte Gower, Mary Ramsay, and Jamie Lopez Bernal. Effectiveness of covid-19 booster vaccines against covid-19-related symptoms, hospitalization and death in england. *Nature medicine*, 28(4):831–837, 2022.

[10] Hiam Chemaitelly, Houssein H Ayoub, Sawsan AlMukdad, Peter Coyle, Patrick Tang, Hadi M Yassine, Hebah A Al-Khatib, Maria K Smatti, Mohammad R Hasan, Zaina Al-Kanaani, et al. Duration of mrna vaccine protection against sars-cov-2 omicron ba. 1 and ba. 2 subvariants in qatar. *Nature Communications*, 13(1):1–12, 2022.

[11] UN. *United Nations World Population Prospects*, 2020. https://population.un.org/wpp/.

[12] Dabo Guan, Daoping Wang, Stephane Hallegatte, Steven J Davis, Jingwen Huo, Shuping Li, Yangchun Bai, Tianyang Lei, Qianyu Xue, D'Maris Coffman, et al. Global supply-chain effects of covid-19 control measures. *Nature human behaviour*, 4(6):577–587, 2020.

[13] Cem Çakmaklı, Selva Demiralp, Ṣebnem Kalemli-Özcan, Sevcan Yesiltas, and Muhammed A Yildirim. Covid-19 and emerging markets: A sir model, demand shocks and capital flows. Technical report, National Bureau of Economic Research, 2020.